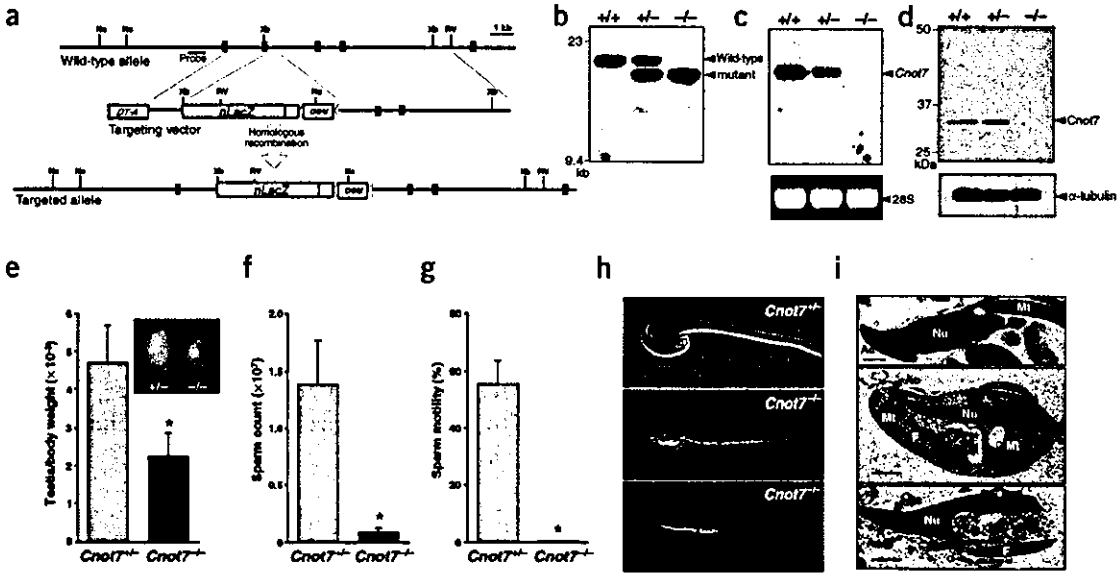

Figure 1 Targeted disruption of *Cnot7* and defects in maturation and morphology of sperm in *Cnot7*$^{-/-}$ mice. (**a**) Schematic diagram of the targeting vector and the wild-type and targeted alleles. Black boxes show exons 2, 3 and 4 of *Cnot7*. *nLacZ*, *lacZ* coding sequence with nuclear localization signal; *neo*, neomycin resistance gene driven by the thymidine kinase promoter; *DT-A*, diphtheria toxin A-chain gene; RV, *Eco*RV; Nc, *Ncol*; K, *Kpnl*; Xh, *Xhol*. (**b**) The 5′ external probe was used for Southern-blot analysis to detect homologous recombination. Tail DNAs from F1 progeny of heterozygote intercrosses were digested with *Ncol* and subjected to Southern-blot hybridization. (**c**) Northern-blot analysis of total RNAs (10 μg) from testes of *Cnot7*$^{+/+}$, *Cnot7*$^{+/-}$ and *Cnot7*$^{-/-}$ mice with the 701-bp fragment (nucleotides 158–858) of the human *CNOT7* cDNA. (**d**) Western-blot analysis of protein extracts from *Cnot7*$^{+/+}$, *Cnot7*$^{+/-}$ and *Cnot7*$^{-/-}$ MEFs with antibodies to Cnot7. (**e**) Comparison of testis weight in three 5-month-old *Cnot7*$^{+/-}$ and *Cnot7*$^{-/-}$ mice. The organs were trimmed free of fat and weighed. (**f**,**g**) Number and motility of sperm prepared from three 5-month-old *Cnot7*$^{+/-}$ and *Cnot7*$^{-/-}$ mice. Sperm counts (**f**) and percentages of motile sperm (**g**) were determined visually by microscopy. Error bars represent s.d. Statistical significance (*$P < 0.01$) in each assay was assessed by Student's *t*-test. (**h**) Morphology of spermatozoa. Spermatozoa were collected from the cauda epididymides of *Cnot7*$^{-/-}$ mice and photographed without fixation under Nomarski optics (magnification, ×600). (**i**) Transmission electron micrographs of spermatozoa from the cauda epididymides in male *Cnot7*$^{+/+}$ (top) and *Cnot7*$^{-/-}$ (middle and bottom) mice. In *Cnot7*$^{+/+}$ mice, head was normally hooked in shape and nucleus (Nu) was condensed. Acrosome (Ac) and mitochondria (Mt) were also normally formed. In *Cnot7*$^{-/-}$ mice, nuclei of spermatozoa were condensed but did not form the characteristic hooked shape. Acrosomes were expanded and attached to nucleus. Abnormal arrangement and localization of mitochondria were apparent and flagella (F) were incorrectly attached. The middle panel shows localization of condensed nucleus in the cytoplasm compartments. The differences in body weight, sperm count, motility and morphology between *Cnot7*$^{+/+}$ and *Cnot7*$^{+/-}$ mice were not significant. Scale bars, 1 μm.

spermatids from *Cnot7*$^{-/-}$ mice into oocytes by conventional ICSI resulted in normal fertilization and production of pups after embryo transfer. The efficiencies were comparable to those after ICSI using control spermatids (**Table 1**), indicating that spermatids from *Cnot7*$^{-/-}$ mice had an adequate set of haploid genome and full oocyte-activating capacity. We conclude from these data that *Cnot7*$^{-/-}$ male germ cells have defects in postmeiotic modifications that are essential for enabling natural delivery of the paternal genome into the oocytes.

Detailed histological analysis of seminiferous tubules from *Cnot7*$^{-/-}$ mice showed a reduction in the number of late spermatids and the presence of large, round, clear vacuoles (**Fig. 2a–g**). In severe cases, most germ cells were lost in seminiferous tubules of *Cnot7*$^{-/-}$ mice (**Fig. 2f**). We often observed multiple generations of elongated spermatids in the same section of seminiferous tubules of *Cnot7*$^{-/-}$ mice (**Fig. 2h**). The data indicate that maturation of spermatids in *Cnot7*$^{-/-}$ mice is unsynchronized. Spermatogenesis in *Cnot7*$^{-/-}$ mice was also distinguished from that in control mice by the presence of syncytial (multinucleated) germ cells (**Fig. 2h**) and a greater number of apoptotic cells (**Fig. 2i,j**). Lipids were unusually accumulated in the cytoplasm of Sertoli cells of adult *Cnot7*$^{-/-}$ mice as compared with control mice (**Fig. 2c,g,k,l**), suggesting that deficiency of Cnot7 induces a metabolic defect in Sertoli cells.

Table 1 ***In vitro*** **and** ***in vivo*** **assessment of fertilizing ability of spermatozoa**

Method	*Cnot7* genotype	Number of oocytes used	Number of oocytes fertilized (%)	Number of embryos transferred	Number of embryos implanted (%)	Number of offspring (%)
IVF	−/−	35	1 (3)[a]	–	–	–
	+/−	23	15 (65)[a]	–	–	–
ICSI	−/−	133	122 (91.2)[b]	110	72 (65.5)[b]	33 (30.0)[b]
	+/+	146	124 (84.9)[b]	124	89 (71.8)[b]	53 (42.7)[b]

[a]$P < 0.01$. [b]$P > 0.05$ (χ^2 test).

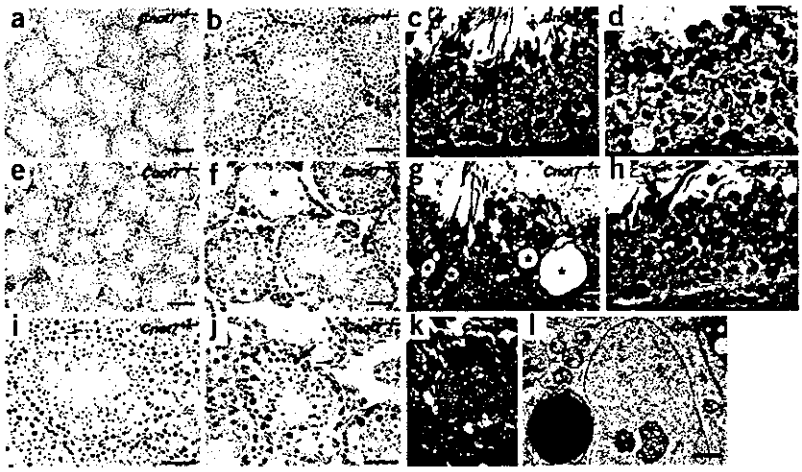

Figure 2 Unusual histology of seminiferous tubules of *Cnot7*$^{-/-}$ mice. (**a**,**b**,**e**,**f**) Histological sections of seminiferous tubules prepared from 5-month-old *Cnot7*$^{+/-}$ (**a**,**b**) and *Cnot7*$^{-/-}$ (**e**,**f**) males were stained with hematoxylin and eosin. Asterisks indicate typical vacuoles. Scale bars: **a**,**e**, 100 μm; **b**,**f**, 50 μm. (**c**,**d**,**g**,**h**) Impairment of sperm maturation in seminiferous tubules of *Cnot7*$^{-/-}$ mice. Histological sections of seminiferous tubules prepared from 2-month-old *Cnot7*$^{+/-}$ (**c**,**d**) and *Cnot7*$^{-/-}$ (**g**,**h**) males were stained with toluidine blue. Asterisks, arrow and filled arrowheads indicate vacuoles, a syncytial cell and unusual accumulations of lipids in the cytoplasm of Sertoli cells, respectively. Spermatogenesis was well-synchronized in *Cnot7*$^{+/-}$ males at stage VIII (**c**) and at stage XII (**d**) but was not well-synchronized in *Cnot7*$^{-/-}$ males at stage VIII (**g**) and at stage XII (**h**), which featured multiple generations of spermatogenic cells (open arrowheads). Double arrowheads in **d** and **h** indicate secondary spermatocytes. Scale bars, 25 μm. (**i**,**j**) More germ cell apoptosis in testes of *Cnot7*$^{-/-}$ mice. Apoptotic cells in seminiferous tubules from 5-month-old *Cnot7*$^{+/-}$ (**i**) and *Cnot7*$^{-/-}$ (**j**) males were stained (brown) intensively by TUNEL. Arrows indicate apoptotic cells. Scale bars, 50 μm. (**k**,**l**) Unusual accumulation of lipids (arrowheads) in the cytoplasm of Sertoli cells. Light micrograph showing spermatogenesis in testis from a *Cnot7*$^{-/-}$ mouse was stained with toluidine blue (**k**). Transmission electron micrograph also shows a lipid droplet in Sertoli cells of testis from a *Cnot7*$^{-/-}$ mouse (**l**). Scale bars: **k**, 10 μm; **l**, 2 μm.

β-galactosidase staining of seminiferous tubules from *Cnot7*$^{+/-}$ mice showed that *Cnot7* was strongly expressed in Sertoli and Leydig cells (Fig. 3a) but only weakly expressed in early round spermatids, spermatocytes and spermatogonia. Because intimate interactions between germ cells and somatic support cells are essential for spermatogenesis, the impaired spermatogenesis in *Cnot7*$^{-/-}$ mice may be caused by defects intrinsic to the support cells. To examine this possibility, we carried out spermatogonial stem cell transplantation[15,16]. We transplanted germ cells from 8- to 10-week-old *Cnot7*$^{-/-}$ males into the seminiferous tubules of WBB6F$_1$ W/W^v (*Kit*$^{W/W\text{-}v}$) mice, busulfan-treated nude (BALB/c) mice or irradiated C57BL/6 mice. The testes of these mice are hospitable for donor cell colonization because they lack endogenous germ cells and have functionally normal Sertoli cells[15]. By tracing expression of the *lacZ* transgene, we found that the transplanted *Cnot7*$^{-/-}$ spermatogonial stem cells differentiated into spermatids in the seminiferous tubules of recipient mice after transplantation (Fig. 3b,c). Morphologically normal spermatids (Fig. 3d) were aligned at the luminal side of seminiferous tubules in the *Kit*$^{W/W\text{-}v}$ recipient testes by 3 months after transplantation (Fig. 3c,e). These results suggest that Cnot7 functions in testicular somatic cells to establish the proper testicular microenvironment for spermatogenesis. Results of reciprocal transplantation experiments, in which germ cells from transgenic mice carrying the pCXN-eGFP transgene[17] were transmitted into the seminiferous tubules of busulfan-treated *Cnot7*$^{-/-}$ mice, were consistent with that conclusion (data not shown).

Several nuclear receptors including estrogen receptor α, androgen receptor, retinoic acid receptor α (Rara) and Rxrb are essential for spermatogenesis[3,18–20]. Of these, Rxrb is expressed in Sertoli and Leydig cells[3,21]. *Rxrb*$^{-/-}$ male mice are sterile, owing to abnormal germ cell maturation that leads to oligo-astheno-teratozoospermia. In addition, Sertoli cells of *Rxrb*$^{-/-}$ mice undergo a progressive accumulation of lipids[3].

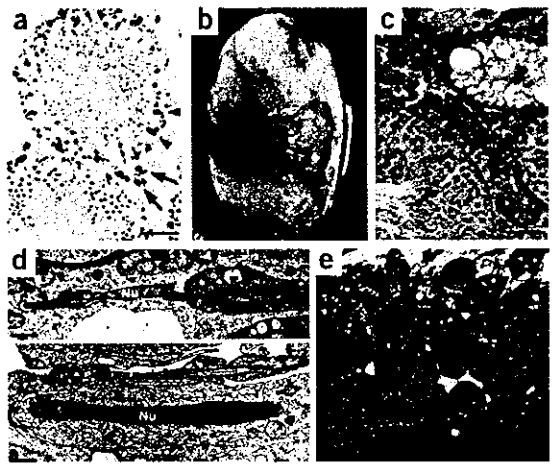

Figure 3 Macroscopic and histological appearances of seminiferous tubules of recipient mouse testes after transplantation of *Cnot7*$^{-/-}$ germ cells. (**a**) Expression of *Cnot7* in testicular cells. β-galactosidase staining of testes from *Cnot7*$^{+/-}$ mice indicates strong *Cnot7* expression in somatic cells. Arrows and arrowheads indicate Leydig and Sertoli cells, respectively. Scale bar, 50 μm. (**b**) A testis from a transplanted recipient mouse showing β-galactosidase expression. β-galactosidase-positive (blue) stretches of seminiferous tubules are colonies from donor spermatogonial stem cells. (**c**) Histological section of *Kit*$^{W/W\text{-}v}$ recipient seminiferous tubules stained with periodic acid–Schiff and hematoxylin. Arrow and arrowhead indicate colonized and noncolonized seminiferous tubules, respectively, after transplantation. Scale bar, 50 μm. (**d**) Transmission electron micrographs showing a malformed head of elongating spermatid in testis of a *Cnot7*$^{-/-}$ mouse (upper panel) and a normally formed head of elongating spermatid obtained from the transplantation experiment (lower panel). Nu, condensed nuclei; Ac, acrosome. Scale bars, 1 μm. (**e**) Histological section of *Kit*$^{W/W\text{-}v}$ recipient seminiferous tubules stained with toluidine blue. Scale bar, 10 μm.

We expressed FLAG-tagged human CNOT7 in COS7 cells together with Rxrb or other nuclear receptors (Rxra, Rxrg, Rara and vitamin D receptor) fused to glutathione S-transferase (GST). GST pull-down assays with the cell lysates showed that CNOT7 interacted only with GST-Rxrb (**Fig. 4a**). This interaction was confirmed by immunoprecipitation experiments with lysates of TTE3 Sertoli cells[22] (**Fig. 4b**). Rxra, Rxrb and Rxrg share a conserved DNA-binding domain (~95% homology) and C-terminal ligand-binding domain (AF-2, ~87% homology). In contrast, the sequence of the N-terminal domain (AF-1), which is involved in autonomous ligand-independent transcriptional activation, is divergent across family members[23]. GST pull-down assays showed that the AF-1 domain of Rxrb interacted with CNOT7 whereas the DNA-binding and AF-2 domains did not (**Fig. 4c**).

We then examined whether Rxrb functions are affected in the absence of Cnot7. To measure the Rxrb-mediated transcription in the *Cnot7*$^{-/-}$ condition, we used primary mouse embryonic fibroblasts (MEFs). We transfected an Rxrb expression vector and a luciferase reporter plasmid containing an RXR response element (RXRE)-coupled thymidine kinase promoter into wild-type or *Cnot7*$^{-/-}$ MEFs. Luciferase reporter assays showed that Rxrb-mediated transcription in response to 9-*cis* retinoic acid was much lower in the absence of Cnot7 (**Fig. 4d**). In addition, electrophoretic mobility shift assays (EMSAs) showed that proteins from testes of *Cnot7*$^{-/-}$ mice bound to the RXRE less efficiently than those from testes of *Cnot7*$^{+/+}$ mice (**Fig. 4e**). Reintroduction of recombinant CNOT7 in the nuclear extracts of testes of *Cnot7*$^{-/-}$ mice resulted in substantial recovery of the ability to bind the RXRE (**Fig. 4f**). Taken together, these findings suggest that the AF-1 domain is responsible for the Rxrb-Cnot7 interaction and that Cnot7 contributes to Rxrb function.

In this study, we found *in vivo* evidence that abnormalities during spermatogenesis in testes of *Cnot7*$^{-/-}$ mice are possibly caused by defects in the testicular somatic cells rather than in the germ cells. The function of testicular somatic cells is directed by pituitary gonadotropins secreted from the hypothalamic-pituitary axis. Among the gonadotropins, luteinizing hormone mainly stimulates testosterone production in the Leydig cells. Because serum testosterone level did not differ between male *Cnot7*$^{+/-}$ and *Cnot7*$^{-/-}$ mice (data not shown), hormonal regulation mediated through the hypothalamic-pituitary axis and Leydig cells seems to be little affected by the absence of Cnot7. The testicular phenotypes in *Cnot7*$^{-/-}$ mice seem to be caused by the functional defect of Sertoli cells.

Although the RXR family members Rxra, Rxrb and Rxrg share structural similarities, genetic analyses suggest that each has distinct roles in mice[24–26]. Our data show that testicular phenotypes of male *Cnot7*$^{-/-}$ mice are similar to those of *Rxrb*$^{-/-}$ mice (vacuole formation, failure in alignment of late spermatids, multiple generations of spermatids, lipid accumulation in the cytoplasm of Sertoli cells and no apparent phenotypic abnormalities in other adult tissues), suggesting that Cnot7 functionally interacts with Rxrb but not with other family members. Indeed, our data show that Rxrb interacts physically and functionally

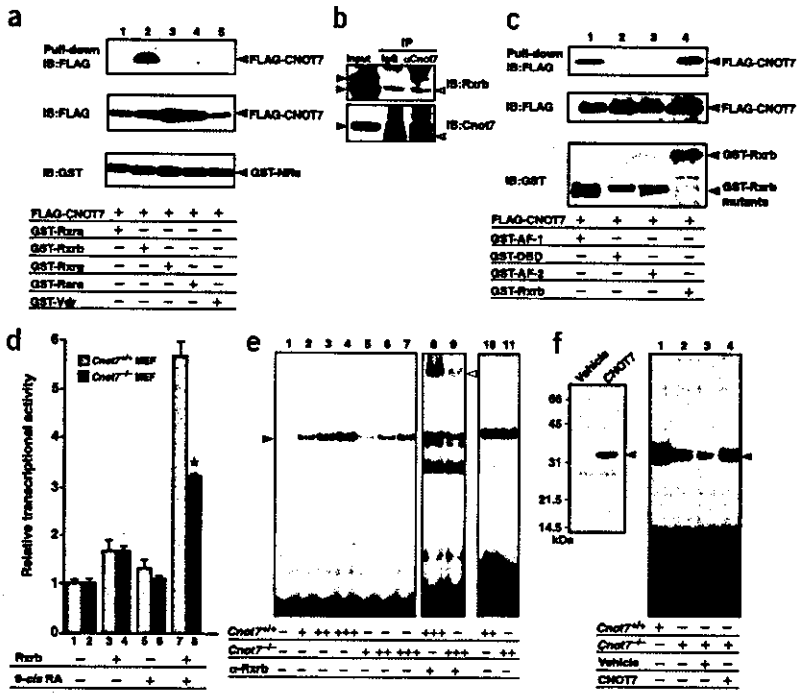

Figure 4 Physical and functional interactions between Cnot7 and Rxrb. (**a**,**c**) FLAG-tagged CNOT7 was coexpressed in COS7 cells with GST-fused nuclear receptors (NRs; mouse Rxra, mouse Rxrb, mouse Rxrg, mouse Rara and rat vitamin D receptor (Vdr); **a**) or GST-fused distinct portions of Rxrb (**c**). Total protein extracts were subjected to GST pull-down assay followed by immunoblotting (IB) with monoclonal antibody against FLAG (top panel). The lower two panels show expression of each indicated protein. (**b**) Proteins in the lysates of TTE3 Sertoli cells were immunoprecipitated with antibodies to Cnot7 (αCnot7) or nonspecific IgG. The immunoprecipitates were subjected to immunoblotting (IB) with antibodies to Rxrb (upper panel) or to Cnot7 (lower panel). Filled arrowheads to the left indicate bands that interacted specifically with antibodies; open arrowheads to the right indicate bands with nonspecific antibody binding. (**d**) Impairment of 9-*cis* retinoic acid (RA)-induced Rxrb-mediated transcription due to the absence of Cnot7. Wild-type and *Cnot7*$^{-/-}$ MEFs were transfected with Rxrb expression plasmid together with RXRE-*luc* reporter plasmid. Cells were incubated in the absence or presence of 9-*cis* retinoic acid (1 μM). Error bars represent s.d. Asterisk indicates a statistically significant difference between wild-type and *Cnot7*$^{-/-}$ MEFs ($P < 0.01$). Statistical differences between groups were assessed by Student's *t*-test. (**e**) Effect of Cnot7 on Rxrb DNA-binding. Increasing amounts of nuclear extracts (1 μg, +; 3 μg, ++; 9 μg, +++) isolated from testes of wild-type (lanes 2–4) or *Cnot7*$^{-/-}$ (lanes 5–7) mice were incubated with a fixed amount of radioactively labeled response element for EMSA. The DNA-binding activity of Rxrb from testes of wild-type mice (lane 8) was compared with that of testes from *Cnot7*$^{-/-}$ mice (lane 9) by supershift experiments with antibody to Rxrb. Levels of Rxrb expression were similar in testes from wild-type and *Cnot7*$^{-/-}$ mice (data not shown). The quantity of nuclear extracts used was confirmed with the oligonucleotide probe containing κB site from the mouse κ-light chain enhancer (lanes 10 and 11). (**f**) Functional associations between Cnot7 and Rxrb. Recombinant CNOT7 was produced in *E. coli* and added to the nuclear extracts of testes from *Cnot7*$^{-/-}$ mice before EMSA (lane 4, right panel). The left panel shows Coomassie brilliant blue staining of the recombinant CNOT7 protein.

with CNOT7 through its AF-1 domain. Therefore, Cnot7 may function as a specific coregulator of Rxrb to contribute to spermatogenesis.

Little is known about the molecular mechanism of human infertility. It may be important to screen men with oligo-astheno-teratozoospermia for polymorphisms or mutations in *CNOT7* to assess whether *CNOT7* has a role in human infertility.

METHODS

Generation of *Cnot7*$^{-/-}$ mice. We subcloned the 18-kb genomic DNA fragment of *Cnot7* into pBluescript. We replaced an exon of *Cnot7* that contains the first methionine with *lacZ* and a *pMC1neo poly(A)* fragment flanked by *lox*P sites to be inserted in-frame with the first methionine to generate the targeting vector. The DT-A fragment was ligated at the 3′ end of the targeting vector for negative selection. We electroporated J1 embryonic stem cells with linearized targeting vector and subjected them to neomycin selection. We identified *Cnot7* targeted clones by Southern-blot hybridization with the probe shown in **Figure 1a**, injected these cells into C57BL/6J blastocysts and mated chimeric offspring with C57BL/6J mice. We intercrossed heterozygous F1 mice to produce homozygous *Cnot7*$^{-/-}$ mice. We carried out all experiments with animals following guidelines for animal use issued by the Committee of Animal Experiments, Institute of Medical Science, University of Tokyo.

Conventional transmission electron microscopy. We fixed adult testes with 2% glutaraldehyde in 0.2 M cacodylate buffer. After washing them in the same buffer, we cut the tissues into small pieces, immersed them in the same fixative for 2 h at 4 °C, rinsed them and fixed them with OsO_4. The samples were dehydrated through graded ethanol and then embedded in Epon 812. We cut ultrathin sections on an ultramicrotome (model Ultracut E, Reihert-Jung) and stained them with uranyl acetate and lead citrate. We observed them with a JEOL 1200 EX (JEOL) transmission electron microscope.

IVF and ICSI. We collected mature oocytes from the oviducts of female B6D2F1 mice that had been superovulated by the injection of 5 IU of equine chorionic gonadotrophin followed 48 h later by 5 IU of human chorionic gonadotropin. We carried out zona-free IVF using epididymal spermatozoa as described[27]. We fixed, stained and examined oocytes by phase-contrast microscopy 2 h after insemination. Oocytes with decondensed sperm nuclei were considered to be fertilized. For ICSI, we collected spermatogenic cells from the seminiferous tubules by a mechanical method and directly injected elongated spermatids at steps 9–11 into oocytes using a Piezo-driven micromanipulator[28]. Oocytes that survived injection were cultured in potassium simplex optimized medium and those developing to the 2-cell stage were transferred into the oviducts of pseudopregnant ICR females. We obtained live offspring at term (day 19.5) by Caesarian section or after natural delivery.

Testes histomorphometry. We fixed testes in Bouin or 10% formalin neutral buffer solution, embedded them in paraffin and cut 7-mm sections. We dewaxed and stained sections with hematoxylin and eosin, with toluidine blue or by PAS reaction with standard procedures.

Analysis of apoptotic cells. We detected apoptotic cells in sections of mouse testes *in situ* by TUNEL assay with an ApopTag peroxidase kit (Intergen). We counterstained sections with diluted hematoxylin.

Production of recipient mice and spermatogonial stem cell transplantation. We obtained male WBB6F$_1$-W/W^v mice from Japan SLC. We injected 6-week-old BALB/cA Jcl-*nu* males (CLEA Japan) intraperitoneally with freshly prepared busulfan (44 mg per kg body weight). Busulfan-treated mice were devoid of endogeneous spermatogenesis at the time of transplantation (~6 weeks after busulfan treatment). We irradiated (12 Gy) the lower halves of the bodies of 14- to 18-d-old C57BL/6N mouse pups (CLEA Japan) to eliminate endogenous germ cells in the testes and used these mice for transplantation experiments 2 d later[29]. We prepared donor cell suspension (2–3 × 10^7 cells ml^{-1}) from 8- to 10-week-old *Cnot7*$^{-/-}$ mice by a two-step enzymatic digestion technique[16] and introduced ~10 µl into the seminiferous tubules of each recipient mouse. We identified donor-derived areas of spermatogenesis in testes of recipients by staining with 5-bromo-4-chloro-3-indolyl β-D-galactoside (X-gal).

Cell culture. We obtained MEFs from 14.5-d-old embryos by an established procedure[14]. We maintained MEFs, COS7 and TTE3 cells in Dulbecco's modified Eagle medium containing 10% fetal bovine serum and antibiotics.

Plasmids. We amplified cDNA fragments for various portions of GST-fused Rxrb by PCR. The AF-1 domain of Rxrb was described previously[30]. Primer sequences for Rxrb mutants are available on request.

GST pull-down. For GST pull-down assays, we lysed cells with RIPA buffer as described[9] 36 h after transfection. We purified GST fusion proteins with glutathione-Sepharose beads, resolved the bound proteins by SDS-PAGE and analyzed them by immunoblotting. Antibodies used for blotting were monoclonal antibody to FLAG (Sigma) and monoclonal antibody to GST (Santa Cruz Biotechnology).

Immunoprecipitation and immunoblotting. We solubilized TTE3 cells in Triton X-100 lysis buffer (0.5% Triton X-100, 50 mM Tris (pH 7.4), 10% glycerol, 100 mM NaCl, 2 mM $MgCl_2$, 0.1 mM $CaCl_2$, 1 µM 9-*cis* retinoic acid and 25 µM MG132) supplemented with protease inhibitor cocktails (Sigma). We incubated precleared lysates sequentially with polyclonal antibodies to Cnot7 and protein A-Sepharose (Amersham Biosciences). We washed the immunoprecipitates at least four times with lysis buffer. We raised rabbit polyclonal antibodies against Cnot7 using a keyhole limpet hemocyanin–conjugated synthetic peptide with the sequence SYVQNGTGNAYEEEANKQS as immunogen and affinity-purified it. We used a monoclonal antibody to Rxrb for blotting, which was a gift from Perseus Proteomics.

Transactivation assay. For Rxrb-mediated transactivation assay, we cotransfected MEFs (5 × 10^4 cells per well in 12-well tissue culture plates) with Lipofectamine (Invitrogen) and the following plasmids: (i) pSG5-Rxrb (0.2 µg), (ii) pGL3-RXRE-Luc (reporter plasmid; 0.05 µg) and (iii) pRL-TK (0.025 µg). We analyzed cell extracts for luciferase activity with a Dual-Luciferase Reporter System (Promega). Transfection efficiency was standardized with an internal control plasmid, pRL-TK. Data are shown as the average ± s.d. of three independent experiments, each done in triplicate.

Preparation of nuclear extracts and EMSA. We isolated testes from 10- to 16-week-old *Cnot7*$^{+/-}$ or *Cnot7*$^{-/-}$ mice, washed them in ice-cold phosphate-buffered saline and suspended them in hypotonic buffer (10 mM HEPES buffer (pH 7.9), 1.5 mM $MgCl_2$, 10 mM KCl, 0.5 mM dithiothreitol (DTT) and 0.2 mM phenylmethylsulfonyl fluoride (PMSF)). We broke cells with ten strokes with a type A Dounce homogenizer and two gentle strokes with a type B Dounce homogenizer. We collected nuclei by centrifugation for 10 min at 600*g* and 4 °C and resuspended them in 500 µl of hypotonic buffer and added 250 µl of low salt buffer (20 mM HEPES buffer (pH 7.9), 25% glycerol, 1.5 mM $MgCl_2$, 20 mM KCl, 0.2 mM EDTA, 0.5 mM DTT and 0.5 mM PMSF). We then added 250 µl of high salt buffer (20 mM HEPES buffer (pH 7.9), 25% glycerol, 1.5 mM $MgCl_2$, 1.2 M KCl, 0.2 mM EDTA, 0.5 mM DTT and 0.5 mM PMSF) dropwise. We extracted nuclei for 30 min at 4 °C with constant rotation, centrifuged the suspension for 30 min at 150,000*g* and 4 °C, collected the supernatant and used it for EMSAs. We used an RXRE composed of two half sites oriented as direct repeats with a 1-kb spacer element as the oligonucleotide probe. We incubated the nuclear extracts at room temperature for 20–30 min with the radioactively labeled oligonucleotide probe (40,000–60,000 c.p.m.) in 15 µl of binding buffer (15 mM Tris-HCl (pH 7.5), 75 mM NaCl, 1.5 mM EDTA, 15 mM DTT, 7.5% glycerol, 1 µg µl^{-1} bovine serum albumin and 0.3% Nonidet P-40). We then resolved the resulting DNA-protein complexes by nondenaturing gel electrophoresis and visualized them by autoradiography. For supershift experiments, we used antibody to Rxrb (Santa Cruz Biotechnology; *sc*-831).

Protein cloning, expression, and purification. We cloned a DNA fragment encoding the full-length human CNOT7 protein into pGEX-6P-3 (Amersham Biosciences). We expressed the protein in *Escherichia coli* BL21, purified it by affinity chromatography on glutathione Sepharose 4B and cleaved it from GST with PreScission protease (Amersham Biosciences). The protein samples from vector-transfected *E. coli* were similarly treated (Vehicle).

Sperm count and motility analysis. We placed cauda epididymides in 0.1 ml of motile buffer (120 mM NaCl, 5 mM KCl, 25 mM $NaHCO_3$, 1.2 mM KH_2PO_4, 1.2 mM $MgSO_4$ and 1.3 mM $CaCl_2$). We minced the tissue with scissors and incubated it at 37 °C for 5 min to allow sperm dispersal.

ACKNOWLEDGMENTS

We thank J. Yanagisawa, Y. Sugitani, T. Nakazawa, M. Ohsugi, T. Tezuka, K. Semba and M. Noda for discussions; S. Kato for providing expression vectors for nuclear receptors and reporter plasmids containing response elements for nuclear receptors; N. Yanai for providing TTE3 cells; and H. Yamanaka, N. Kusaka, A. Nakamura, M. Yoneda, A. Moriya and F. Suzuki-Toyota for technical support. This work was supported by a Grant for Advanced Cancer Research from the Ministry of Education, Science, Sports, and Culture of Japan and grants from the Organization for Pharmaceutical Safety and Research of Japan, and from the Research Fellowships of the Japan Society for the Promotion of Science for Young Scientists.

COMPETING INTERESTS STATEMENT

The authors declare that they have no competing financial interests.

Received 21 January; accepted 17 March 2004
Published online at http://www.nature.com/naturegenetics/

1. Matzuk, M.M. & Lamb, D.J. Genetic dissection of mammalian fertility pathways. *Nat. Cell Biol.* **4** Suppl, S41–S49 (2002).
2. Prevot, D. *et al.* Relationships of the antiproliferative proteins BTG1 and BTG2 with CAF1, the human homolog of a component of the yeast CCR4 transcriptional complex: involvement in estrogen receptor alpha signaling pathway. *J. Biol. Chem.* **276**, 9640–9648 (2001).
3. Kastner, P. *et al.* Abnormal spermatogenesis in RXRβ mutant mice. *Genes Dev.* **10**, 80–92 (1996).
4. Draper, M.P., Salvadore, C. & Denis, C.L. Identification of a mouse protein whose homolog in Saccharomyces cerevisiae is a component of the CCR4 transcriptional regulatory complex. *Mol. Cell. Biol.* **15**, 3487–3495 (1995).
5. Collart, M.A. Global control of gene expression in yeast by the Ccr4-Not complex. *Gene* **313**, 1–16 (2003).
6. Denis, C.L. & Chen, J. The CCR4-NOT complex plays diverse roles in mRNA metabolism. *Prog. Nucleic Acid Res. Mol. Biol.* **73**, 221–250 (2003).
7. Rouault, J.P. *et al.* Interaction of BTG1 and p53-regulated BTG2 gene products with mCaf1, the murine homolog of a component of the yeast CCR4 transcriptional regulatory complex. *J. Biol. Chem.* **273**, 22563–22569 (1998).
8. Albert, T.K. *et al.* Isolation and characterization of human orthologs of yeast CCR4-NOT complex subunits. *Nucleic Acids Res.* **28**, 809–817 (2000).
9. Ikematsu, N. *et al.* Tob2, a novel anti-proliferative Tob/BTG1 family member, associates with a component of the CCR4 transcriptional regulatory complex capable of binding cyclin-dependent kinases. *Oncogene* **18**, 7432–7441 (1999).
10. Yoshida, Y., Hosoda, E., Nakamura, T. & Yamamoto, T. Association of ANA, a member of the antiproliferative Tob family proteins, with a Caf1 component of the CCR4 transcriptional regulatory complex. *Jpn. J. Cancer Res.* **92**, 592–596 (2001).
11. Prevot, D. *et al.* The leukemia-associated protein Btg1 and the p53-regulated protein Btg2 interact with the homeoprotein Hoxb9 and enhance its transcriptional activation. *J. Biol. Chem.* **275**, 147–153 (2000).
12. Yoshida, Y. *et al.* Negative regulation of BMP/Smad signaling by Tob in osteoblasts. *Cell* **103**, 1085–1097 (2000).
13. Tzachanis, D. *et al.* Tob is a negative regulator of activation that is expressed in anergic and quiescent T cells. *Nat. Immunol.* **2**, 1174–1182 (2001).
14. Yoshida, Y. *et al.* Mice lacking a transcriptional corepressor Tob are predisposed to cancer. *Genes Dev.* **17**, 1201–1206 (2003).
15. Brinster, R.L. & Zimmermann, J.W. Spermatogenesis following male germ-cell transplantation. *Proc. Natl. Acad. Sci. USA* **91**, 11298–11302 (1994).
16. Ogawa, T., Dobrinski, I., Avarbock, M.R. & Brinster, R.L. Transplantation of male germ line stem cells restores fertility in infertile mice. *Nat. Med.* **6**, 29–34 (2000).
17. Ogawa, T., Ohmura, M., Yumura, Y., Sawada, H. & Kubota, Y. Expansion of murine spermatogonial stem cells through serial transplantation. *Biol. Reprod.* **68**, 316–322 (2003).
18. Lufkin, T. *et al.* High postnatal lethality and testis degeneration in retinoic acid receptor α mutant mice. *Proc. Natl. Acad. Sci. USA* **90**, 7225–7229 (1993).
19. Eddy, E.M. *et al.* Targeted disruption of the estrogen receptor gene in male mice causes alteration of spermatogenesis and infertility. *Endocrinology* **137**, 4796–4805 (1996).
20. Charest, N.J. *et al.* A frameshift mutation destabilizes androgen receptor messenger RNA in the Tfm mouse. *Mol. Endocrinol.* **5**, 573–581 (1991).
21. Livera, G., Rouiller-Fabre, V., Pairault, C., Levacher, C. & Habert, R. Regulation and perturbation of testicular functions by vitamin A. *Reproduction* **124**, 173–180 (2002).
22. Tabuchi, Y. *et al.* Development of the conditionally immortalized testicular Sertoli cell line TTE3 expressing Sertoli cell specific genes from mice transgenic for temperature sensitive simian virus 40 large T antigen gene. *J. Urol.* **167**, 1538–1545 (2002).
23. Mangelsdorf, D.J. *et al.* Characterization of three RXR genes that mediate the action of 9-cis retinoic acid. *Genes Dev.* **6**, 329–344 (1992).
24. Sucov, H.M. *et al.* RXRα mutant mice establish a genetic basis for vitamin A signaling in heart morphogenesis. *Genes Dev.* **8**, 1007–1018 (1994).
25. Kastner, P. *et al.* Genetic analysis of RXRα developmental function: convergence of RXR and RAR signaling pathways in heart and eye morphogenesis. *Cell* **78**, 987–1003 (1994).
26. Krezel, W. *et al.* RXRγ null mice are apparently normal and compound $RXR\alpha^{-/-}/RXR\beta^{-/-}/RXR\gamma^{-/-}$ mutant mice are viable. *Proc. Natl. Acad. Sci. USA* **93**, 9010–9014 (1996).
27. Maleszewski, M., Kimura, Y. & Yanagimachi, R. Sperm membrane incorporation into oolemma contributes to the oolemma block to sperm penetration: evidence based on intracytoplasmic sperm injection experiments in the mouse. *Mol. Reprod. Dev.* **44**, 256–259 (1996).
28. Ogonuki, N. *et al.* Fertilization of oocytes and birth of normal pups following intracytoplasmic injection with spermatids in mastomys (Praomys coucha). *Biol. Reprod.* **68**, 1821–1827 (2003).
29. Creemers, L.B. *et al.* Transplantation of germ cells from glial cell line-derived neurotrophic factor-overexpressing mice to host testes depleted of endogenous spermatogenesis by fractionated irradiation. *Biol. Reprod.* **66**, 1579–1584 (2002).
30. Leid, M. *et al.* Purification, cloning, and RXR identity of the HeLa cell factor with which RAR or TR heterodimerizes to bind target sequences efficiently. *Cell* **68**, 377–395 (1992).

Spermatogenesis from epiblast and primordial germ cells following transplantation into postnatal mouse testis

Shinichiro Chuma[1], Mito Kanatsu-Shinohara[2], Kimiko Inoue[3], Narumi Ogonuki[3], Hiromi Miki[3], Shinya Toyokuni[4], Mihoko Hosokawa[1], Norio Nakatsuji[1], Atsuo Ogura[3] and Takashi Shinohara[2,*]

[1]Department of Development and Differentiation, Institute for Frontier Medical Sciences, Kyoto University, Kyoto 606-8507, Japan
[2]Horizontal Medical Research Organization, Graduate School of Medicine, Kyoto University, Kyoto 606-8501, Japan
[3]The Institute of Physical and Chemical Research (RIKEN), Bioresource Center, Ibaraki 305-0074, Japan
[4]Department of Pathology and Biology of Diseases, Graduate School of Medicine, Kyoto University, Kyoto 606-8501, Japan
*Author for correspondence (e-mail: takashi@mfour.med.kyoto-u.ac.jp)

Accepted 27 October 2004

Development 132, 117-122
Published by The Company of Biologists 2005
doi:10.1242/dev.01555

Summary

Primordial germ cells (PGCs) are derived from a population of pluripotent epiblast cells in mice. However, little is known about when and how PGCs acquire the capacity to differentiate into functional germ cells, while keeping the potential to derive pluripotent embryonic germ cells and teratocarcinomas. In this investigation, we show that epiblast cells and PGCs can establish colonies of spermatogenesis after transfer into postnatal seminiferous tubules of surrogate infertile mice. Furthermore, we obtained normal fertile offspring by microinsemination using spermatozoa or spermatids derived from PGCs harvested from fetuses as early as 8.5 days post coitum. Thus, fetal male germ cell development is remarkably flexible, and the maturation process, from epiblast cells through PGCs to postnatal spermatogonia, can occur in the postnatal testicular environment. Primordial germ cell transplantation techniques will also provide a novel tool to assess the developmental potential of PGCs, such as those manipulated in vitro or recovered from embryos harboring lethal mutations.

Key words: Germ cell, Epiblast, Primordial Germ Cell (PGC), Pro-spermatogonia, Spermatogonia, Testis, Spermatogenesis, Transplantation, Microinsemination

Introduction

Mammalian germ cells undergo unique genetic and cellular changes as they develop and differentiate to form functional gametes. A population of pluripotent epiblast cells at around 6.5 days post coitum (dpc) gives rise to primordial germ cells (PGCs), which become identifiable as a cluster of cells at the base of the allantois at 7.25 dpc (Ginsburg et al., 1990; Tam and Zhou, 1996; Tsang et al., 2001). During development, the number of PGCs increases from 40 cells at 7.5 dpc to 25,000 cells at 13.5 dpc, and they migrate through the developing hindgut and mesentery to reach the urogenital ridge (UGR) at around 10.5 dpc. By 13.5 dpc, PGCs in the male genital ridge enter into mitotic arrest and become pro-spermatogonia, while germ cells in the female arrest at meiotic prophase I (reviewed by McLaren, 2003). Primordial germ cells show different features at different developmental stages. For example, migratory-stage PGCs exhibit a higher frequency of conversion into embryonic germ cells, pluripotent cells that resemble blastocyst-derived embryonic stem cells, than do PGCs in the gonads (Matsui et al., 1992; Resnick et al., 1992; Labosky et al., 1994). In addition, epigenetic changes characteristic to germline cells also occur in PGCs. Erasure of parental genomic imprints on both paternal and maternal alleles in PGCs commences near the time of their settlement in the UGR at 10.5 dpc, and new imprints are imposed in pro-spermatogonia before birth (Szabo and Mann, 1995; Ueda et al., 2000; Surani, 2001; Hajkova et al., 2002). Therefore, the characteristics of PGCs change during development before they mature into postnatal germ cells.

Spermatogenesis is initiated shortly after birth (Russell et al., 1990; Meistrich and van Beek, 1993). Pro-spermatogonia resume mitosis as spermatogonia, at around postnatal day 5, then enter into meiosis as spermatocytes and produce spermatids, which develop into spermatozoa. Spermatogonial stem cells are a subpopulation of spermatogonia and have the unique ability to self-renew as well as to differentiate to produce spermatozoa (Meistrich and van Beek, 1993; de Rooij and Russell, 2000). These cells continue to divide throughout the life of the animal, and can be identified by their ability to generate and maintain colonies of spermatogenesis following transplantation into the seminiferous tubules of infertile recipient testes (Brinster and Zimmermann, 1994). Using this assay, several groups have shown that pro-spermatogonia in developing fetal testes can differentiate into spermatogonial stem cells when transferred into the adult testis (Ohta et al., 2004; Jiang and Short, 1998). However, it is unknown if germline cells at earlier stages of development can produce spermatogonial stem cells or spermatogenic colonies after transplantation.

In this investigation, we sought to determine the potential of germline cells from earlier embryos to develop into spermatogonial stem cells, using immature recipient animals.

Epiblast cells or PGCs were transplanted into infertile mouse testes and examined for their ability to re-populate the seminiferous tubules.

Materials and methods

Collection of donor cells

Donor cells were collected from pregnant C57BL/6 mice that were maintained in a controlled environment with 12:12 light:dark cycles from 08.00 h to 20.00 h (SLC, Shizuoka, Japan). The day when a copulation plug was found was designated as 0.5 dpc. In some experiments, we used a transgenic mouse line C57BL/6 Tg14 (act-EGFP) OsbY01 (designated Green) provided by Dr M. Okabe (Osaka University, Osaka, Japan) (Okabe et al., 1997). The spermatogonia, spermatocytes and round spermatids of these mice express the enhanced green fluorescent protein (EGFP) gene, which gradually decreases after meiosis. The sex of embryos was determined using genotyping based on the *Ube1* PCR method (Chuma and Nakatsuji, 2001), and only male embryos were used in this study. Due to the limitations of cell recovery and the number of animals that could be injected per day, the sex check was not performed in experiments using 6.5 dpc embryos. Cells for transplantation were obtained from whole embryonic ectoderm with primitive endoderm at 6.5 dpc, or germ-cell-containing tissues by dissection of the posterior thirds of 8.5 dpc embryos, the mesenteries and guts of 10.5 dpc embryos, the UGRs of 10.5 dpc embryos, and the genital ridges of 11.5, 12.5, 14.5 and 16.5 dpc embryos. Tissues from each developmental stage were dissociated by enzymatic digestion using 0.25% trypsin with 1 mmol/l EDTA (Invitrogen, Carlsbad, CA) for 10 minutes. Cells were suspended in Dulbecco's modified Eagle's medium, supplemented as previously described (Ogawa et al., 1997).

Transplantation into recipient testes

Donor cells were transplanted in histocompatible W/W^v or W^v/W^v mice (*W* mice, obtained from SLC, Shizuoka, Japan). Only 5- to 10-day-old male mice were used as recipients. *W* mutants lack endogenous spermatogenesis (Silvers, 1979), because of mutations in the *Kit* gene (Nocka et al., 1990; Hayashi et al., 1991). Recipient animals were placed on ice to induce hypothermic anesthesia, and returned to their dams after surgery (Shinohara et al., 2001). Approximately 2 μl of cell suspension were introduced into each testis by injection via the efferent duct (Ogawa et al., 1997).

Histological analysis

Three to four months after transplantation, the recipient testes were fixed in 10% neutral-buffered formalin (Wako Pure Chemical Industries, Osaka, Japan) and processed for paraffin sectioning. Sections were stained with hematoxylin and eosin. Two histological sections were prepared from the testes of each animal and viewed at 400× magnification to determine the extent of spermatogenesis. The numbers of tubule cross-sections with or without spermatogenesis (defined as the presence of multiple layers of germ cells in the seminiferous tubule) were recorded for one histological section from each testis. Meiosis was detected by immunofluorescence staining using anti-synaptonemal complex protein 3 (SCP3) antibody (Chuma and Nakatsuji, 2001) and Alexa 488-conjugated anti-rabbit immunoglobulin G antibody (Molecular Probes, Eugene, USA). Periodic acid Schiff (PAS) staining (Muto Pure Chemicals, Tokyo, Japan) was carried out to examine acrosome formation in spermatids. In experiments using Green mice, recipient testes were recovered 10 to 11 weeks after donor cell transplantation, and analyzed by observing EGFP signals under fluorescence microscopy. Donor cells were identified specifically because host testis cells had no endogenous fluorescence. A cluster of germ cells was defined as a colony when it occupied the entire circumference of the tubule and was at least 0.1 mm long (Nagano et al., 1999). Cryosections of the testes fixed in 4% paraformaldehyde in PBS were stained with Rhodamine-conjugated Peanut agglutinin (PNA) (Vector, Burlingame, CA) for acrosomes, and with Hoechst 33258 (Sigma, St Louis, MO) for nuclei.

Microinsemination

Microinsemination was undertaken by intracytoplasmic injection into C57BL/6 × DBA/2 F1 oocytes (Kimura and Yanagimachi, 1995). Embryos that were constructed using spermatozoa or elongated spermatids derived from 8.5 dpc or 12.5 dpc PGCs were transferred into the oviducts of pseudopregnant ICR females after 24 or 48 hours in culture, respectively. Live fetuses retrieved on day 19.5 were raised by lactating ICR foster mothers.

Genotyping of offspring and bisulfite sequencing of imprinted genes

PCR fragments of the *Kit* gene encompassing the *W* point mutation or the W^v mutation (Nocka et al., 1990; Hayashi et al., 1991) were amplified using genomic DNA from mice derived from PGC transplantation, or from a W/W^v mouse as a control heterozygote for both mutations. PCR primers were 5′-CATTTATCTCCTCGACAAC-CTTCC-3′ and 5′-GCTGCTGGCTCACAATCATGGTTC-3′ for *W* genotyping, and 5′-AGATGGCAACTCGAGACTCACCTC-3′ and 5′-TGCCCCCACGCTTTGTTTTGCTAA-3′ for W^v genotyping. Amplified products were gel extracted and directly sequenced.

Bisulfite genomic sequencing of differentially methylated regions (DMRs) of the *Igf2r* and *H19* imprinted genes was carried out as described (Ueda et al., 2000; Lee et al., 2002; Lucifero et al., 2002). Briefly, genomic DNAs were isolated from the offspring derived from PGC transplantation, and treated with sodium bisulfite, which deaminates unmethylated cytosines to uracils, but does not affect 5-methylated cytosines. Polymerase chain reaction amplification of each DMR from bisulfite-treated genomic DNAs was carried out using primer sets as described (Ueda et al., 2000; Lucifero et al., 2002), and DNA sequences were determined.

Results

Epiblasts with primitive endoderms (6.5 dpc) or tissues containing fetal germ cells were collected from different stages of embryos (posterior third of 8.5 dpc embryos, mesenteries and guts of 10.5 dpc embryos, or gonads of 10.5 to 16.5 dpc embryos) (Fig. 1A). The cells were dissociated enzymatically and single cell suspensions were transplanted into the seminiferous tubules of recipient immature *W* mice. Although *W* mice have a very small number of spermatogonia (Ohta et al., 2003), spermatogenesis is arrested at the point of undifferentiated type A spermatogonia and no differentiating germ cells are found due to defects in the *Kit* gene (Nocka et al., 1990; Hayashi et al., 1991) (Fig. 1B). Therefore, any spermatogenesis detected in the recipient testis must be derived from the donor cells. Although the concentration of cells injected varied due to the more limited recovery of cells from early-stage fetuses, the cell viability, or percentage of tubules filled with donor cells, was similar in all experiments. The recipient mice were sacrificed 3 to 4 months after transplantation, and the testes were examined histologically for the presence of spermatogenesis. This time period represents three to four spermatogenic cycles in mice (Meistrich and van Beek, 1993; de Rooij and Russell, 2000), which would allow sufficient time for the development of sperm from spermatogonial stem cells.

At least three experiments were performed using cells harvested from each stage of embryonic development, and the

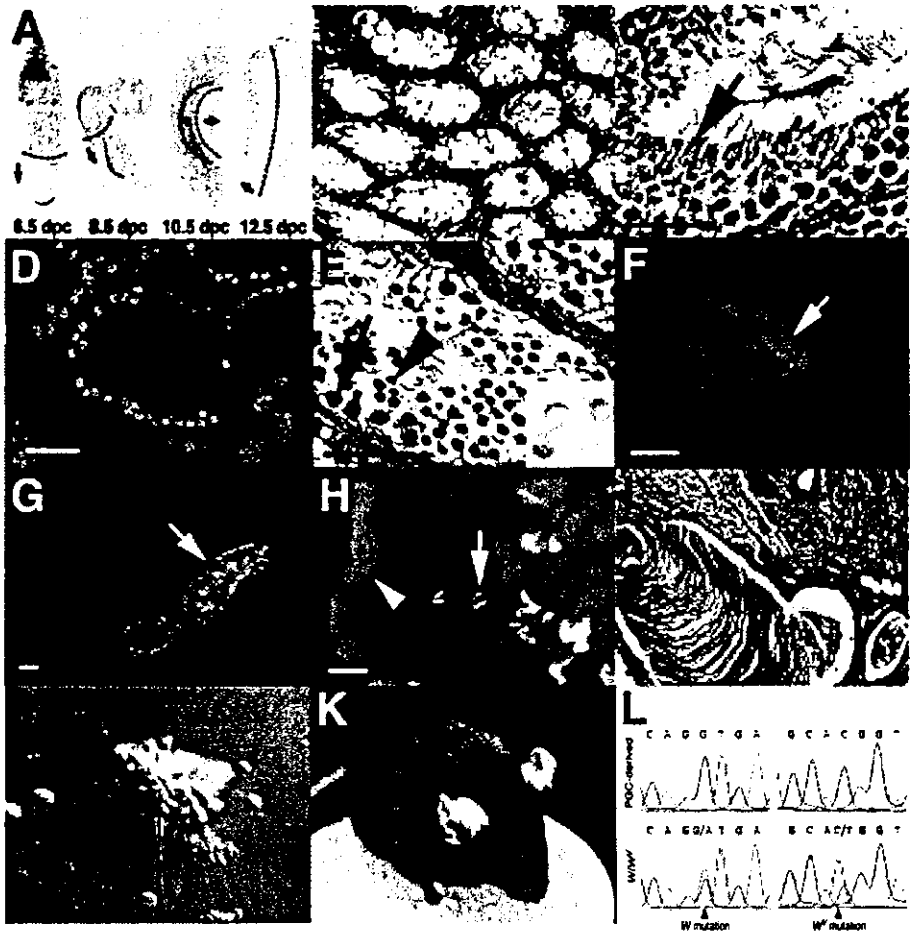

Fig. 1. Spermatogenesis and teratogenesis from fetal germ cells and epiblast cells. (A) Embryos at 6.5 and 8.5 dpc, a mid-part of 10.5 dpc embryo, and a male gonad and mesonephros at 12.5 dpc. Dotted lines demarcate regions used for transplantation. At 10.5 dpc, the urogenital ridges (asterisk) and mesentery with gut (arrow) were dissected separately. (B) A section of a *W* male testis (control recipient) stained with HE. Spermatogenesis is absent. (C) *W* mouse testis after transplantation of 8.5 dpc PGCs. Spermatozoa (arrow) are present in the center of the seminiferous tubule. (D) Anti-SCP3 immunostaining (green) of *W* testis after transplantation of 8.5 dpc PGCs, counterstained with Hoechst 33258 dye (blue). Inset, higher magnification view of the same sample. (E) Transplantation of epiblast cells at 6.5 dpc. Spermatocyte (arrow) and round spermatid (arrow head) were found. Inset shows acrosomes stained with PAS (red) in round spermatids. (F) *W* mouse testis transplanted with 8.5 dpc PGCs from Green mice embryos. Colonization of the recipient seminiferous tubule by EGFP (+) donor cells (green) was observed (arrow). (G) A section of the same testis as in (F), stained with Rhodamine-PNA (red) for acrosomes and with Hoechst 33258 dye (blue) for nuclei. Spermatogenenic colonies derived from EGFP (+) donor cells are present (arrow). (H) Higher magnification view of (G), showing spermatogonia (arrowhead) residing at the base of the seminiferous tubule, and elongated spermatids (arrow) with acrosomes (red), shedding the EGFP (+) cytoplasm. (I) Teratoma from epiblast cells at 6.5 dpc. Muscle, dermoid cyst and neuronal tissue are observed. (J) Spermatozoa (arrow) clustered around a Sertoli cell, released from a recipient testis of 8.5 dpc PGCs. (K) An offspring developed from an oocyte injected with a sperm derived from 8.5 dpc PGCs. (L) DNA sequences of the *Kit* gene around the *W* (left panels) and W^v (right panels) point mutations of an offspring derived from transplantation of 8.5 dpc PGCs (upper panels) and a W/W^v mouse as a control heterozygote (lower panels). Scale bars: 1 mm in F; 10 μm in H; 20 μm in J; 50 μm in others.

Table 1. Donor cell colonization in *W* recipient mice

Donor age (dpc)	Number of recipient testes	Number of transplanted cells ($\times 10^4$/testis)	Number of testes with spermatogenesis (%)	% tubule cross-section with spermatogenesis*	Number of testes with teratoma (%)
6.5	27	0.4±0.2	2 (7.4)	0.1±0.1	4 (14.8)
8.5	13	7.2±0.6	9 (69.2)	3.8±0.1	4 (30.8)
10.5 (mes+gut)	12	12.8±1.4	4 (33.3)	0.9±0.5	0
10.5 (UGR)	15	11.4±2.4	11 (73.3)	7.2±0.1	0
11.5	13	2.4±1.0	8 (61.5)	2.4±0.7	0
12.5	13	9.0±1.6	11 (84.6)	15.7±4.5	0
14.5	12	20	12 (100)	56.5±10.8	0
16.5	12	20	12 (100)	59.3±7.5	0

Values are mean±s.e.m. Results from at least three separate experiments. Testes were analyzed 3-4 months after transplantation. Mes+gut, mesentery and gut; UGR, urogenital ridge.
*Percentage of tubule cross-sections containing spermatogenesis/total tubule cross-sections examined in each testis.

results are summarized in Table 1. Overall, 69 of 117 (59%) recipient testes showed spermatogenesis, but no differentiating germ cells were found in control testes that did not receive an injection of donor cells (Fig. 1B). Spermatogenesis observed in the recipient testes originated from spermatogonial stem cells, because other spermatogenic cells do not have the

Table 2. Development of oocytes injected with spermatogenic cells derived from PGCs

Donor age (dpc)	Number of reconstituted eggs	In vitro development (%)			Number of eggs transferred	Implantation sites (%)	Number of offspring (%)
		One cell	Two cell	Four cell			
8.5*	186	78 (41.9)	105 (56.5)	NA†	105	47 (25.2)	20 (10.8)
12.5	182	8 (4.4)	25 (13.7)	130 (71.4)	130	88 (48.3)	29 (15.9)

Combined results using elongated spermatids and spermatozoa.
*Combined results from two different recipient testes.
†NA, not applicable because cells were transferred at the two-cell stage.

capacity for self-renewal and disappear by 35 days after transplantation (Russell et al., 1990; Brinster and Zimmermann, 1994; Shinohara et al., 2001). Spermatogenesis in the recipient testes that received fetal germ cells (8.5-16.5 dpc) was morphologically normal (Fig. 1C), and the kinetics of spermatogenic colonization were generally comparable to results obtained after transplantation of postnatal spermatogonial stem cells (Shinohara et al., 2001). All stages of spermatogenic cells, including mature spermatozoa, were found in recipient testes. Synchrony of meiosis in seminiferous tubules was confirmed by immunostaining for SCP3, a component of the synaptonemal complex (Fig. 1D).

The age of the donors had a significant effect on the number of recipient seminiferous tubules with observable spermatogenesis. Whereas only 0 to 11% of the tubules showed spermatogenesis in testes that received 8.5 dpc PGCs, spermatogenesis derived from donor cells at later stages of gonadal development was generally more extensive, and recipient testes grew larger due to the increased production of germ cells. In one case, transplantation of 16.5 dpc pro-spermatogonia resulted in 96% of the tubules with evident spermatogenesis, and spermatozoa were transported to the epididymis (data not shown). Spermatogenesis was also found in the recipients that were injected with cells from epiblasts with primitive endoderms. Although we could not identify mature spermatozoa histologically, spermatogenesis was found in two different testes that received injections of 6.5 dpc epiblast and primitive endoderm cells. The spermatogonia, spermatocytes and round spermatids that developed in the recipient seminiferous tubules appeared morphologically normal (Fig. 1E), and acrosome formation in round spermatids was confirmed by PAS staining (Fig. 1E, inset).

To confirm the donor origin of spermatogenesis, we used Green mice that ubiquitously express the *EGFP* transgene. Donor cells were collected from the posterior thirds of 8.5 dpc embryos that showed EGFP signals. This allowed specific identification of donor cells, because endogenous host testis cells had no detectable fluorescence. Four experiments were performed, and a total of 16 testes were microinjected with donor cells. Approximately 6 to 12 $\times$ 10^3 cells were transplanted into each testis. When the recipients were analyzed 10 to 11 weeks after transplantation, 4 of 16 (25%) testes had spermatogenic colonies that showed EGFP signals (Fig. 1F). The average number of colonies per testis was 0.3 ± 0.1 (mean ± s.e.m.). Histological analysis of the EGFP (+) colonies showed the presence of apparently normal spermatogenesis (Fig. 1G,H).

While these results indicate that all types of donor cells differentiated into spermatogonial stem cells, differentiation of donor cells was not restricted to the germline lineage. Consistent with findings of previous studies (Illmensee and Stevens, 1979), testes receiving epiblast cells or 8.5 dpc PGCs formed teratomas (Fig. 1I). Epiblast cells produced larger tumors than did 8.5 dpc PGCs, and some of the seminiferous

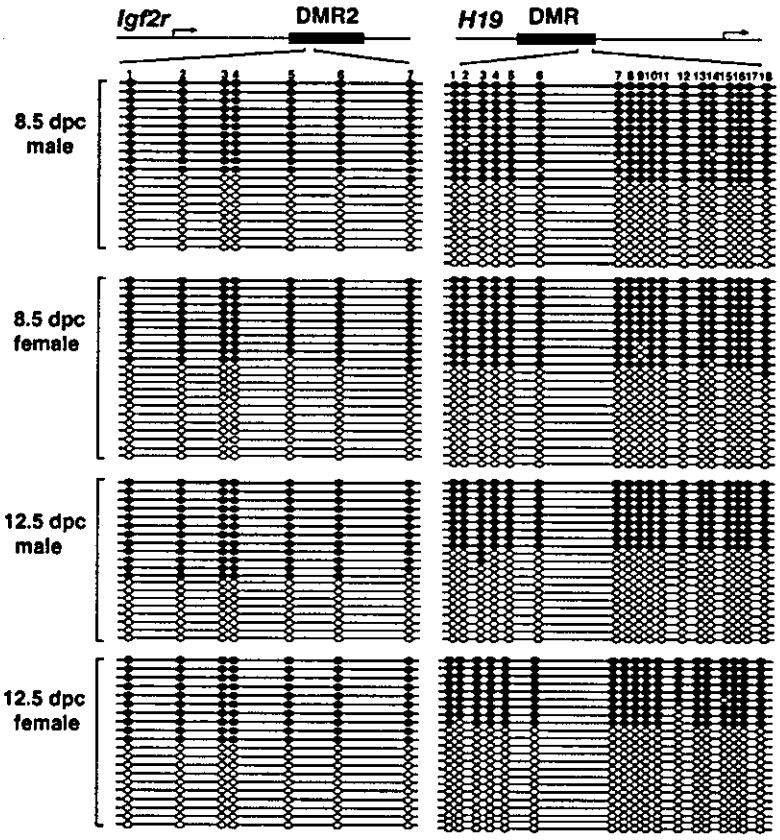

Fig. 2. DMR methylation of the *Igf2r* and *H19* genes in offspring derived from transplantation of 8.5 and 12.5 dpc PGCs. DNA methylation was analyzed by bisulfite genomic sequencing. Both male and female offspring of each stage of donor PGCs were analyzed. Individual lines represent sequenced clones. Black ovals indicate methylated cytosine-guanine sites (CpGs) and white ovals indicate unmethylated CpGs.

tubules were dilated and broken. Cells from three germ layers, including ciliated epithelium, muscle, neuron and bone, were found in these testes. Interestingly, spermatogenesis was occasionally observed in tubules not affected by tumorigenesis, indicating that the same population of donor cells could cause spermatogenesis and teratogenesis. No teratomas were found in the recipients of gonadal PGCs or pro-spermatogonia.

To examine whether germ cells generated from PGCs were fully functional, we performed microinsemination, a technique commonly used to produce offspring from infertile animals and humans (Kimura and Yanagimachi, 1995; Palermo et al., 1992). Donor PGCs were collected from 8.5 or 12.5 dpc embryos, and transplanted into the testes of *W* mice. Four months after transplantation, spermatozoa or elongated spermatids were collected from tubule fragments by mechanical dissociation (Fig. 1J), and microinjected into oocytes. The results of the microinsemination experiments are summarized in Table 2. Spermatogenic cells derived from 8.5 dpc PGCs appeared to be less competent for egg activation, because a significant number of eggs receiving elongated spermatid/spermatozoa from 8.5 dpc PGCs stayed at metaphase II or the metaphase II-anaphase transition and did not develop into the 2-cell stage after 24 hours. However, offspring were obtained from oocytes inseminated with spermatid/spermatozoa derived from both stages of PGCs (Fig. 1K). Genotyping of offspring showed that they did not carry *W* or W^v mutations in the *Kit* gene (Nocka et al., 1990; Hayashi et al., 1991), demonstrating the offspring were derived from wild-type donor PGCs that had been transplanted into the testis (Fig. 1L). No apparent abnormality was seen in any of the offspring, and they were fertile. Bisulfite sequencing analysis of the offspring showed no obvious fluctuations in the methylation status of the DMRs of paternally methylated *H19* and maternally methylated *Igf2r* genes (Fig. 2).

Discussion

This study demonstrates that not only migrating PGCs but also epiblast cells can differentiate into spermatogonial stem cells and produce spermatogenesis after transfer into postnatal testis. The ability to initiate and maintain spermatogenesis after transfer into the infertile testis fulfills the criteria for the identification of spermatogonial stem cells (Brinster and Zimmermann, 1994). Developmental processes that occur during differentiation of spermatogonial stem cells from epiblast cells include induction of PGCs among epiblast cells, migration and proliferation of PGCs, erasure of parental genomic imprints, and G1 (G0) arrest in the developing male gonad. Nonetheless, our results demonstrate that these developmental events do not necessarily require embryonic somatic environments, and most processes of male germline differentiation can take place in postnatal testis. This flexibility of fetal germ cell differentiation may be related to, and partly account for, the recent success in the derivation of sperm from embryonic stem cells in vitro (Toyooka et al., 2003; Geijsen et al., 2004).

The important factor that contributed to the results of our experiments is the use of immature postnatal testes as recipients. Recently, Ohta et al. (Ohta et al., 2004) showed that pro-spermatogonia from 14.5 dpc embryos completed spermatogenesis when transplanted in mature seminiferous tubules, while spermatogenesis did not occur from PGCs from 12.5 dpc embryos. Another group reported that germ cells from day 0-3 mouse pups did not show spermatogenic colonies after transplantation into adult testes (McLean et al., 2003). In our study, however, epiblast cells at 6.5 dpc and PGCs at 8.5 to 16.5 dpc produced spermatogenesis after transplantation into immature seminiferous tubules at postnatal day 5 to 10. This difference might simply be ascribed to structural differences; immature Sertoli cells lack tight junctions and may allow migrating transplanted cells easier access to the stem cell niches, which are distributed nonrandomly in the seminiferous tubules (Chiarini-Garcia et al., 2001). Alternatively, immature testis may express factors that support survival and differentiation of epiblast cells and PGCs, while mature testis may not. Because PGCs have chemotaxic activity (Godin et al., 1990), we speculate that some of the transplanted cells migrated into the niches of immature seminiferous tubules, where they could survive. PGCs and epiblast cells may have then switched their cell cycle fate to function as spermatogonial stem cells. Both male and female PGCs enter into meiosis in the absence of the male gonadal environment, but do not if they lodge there (McLaren and Southee, 1997; Chuma and Nakatsuji, 2001). Somatic cells in the fetal testis are assumed to produce a substance that inhibits the meiotic transition of PGCs. Given our results, it appears that seminiferous tubules of newborn mice may also have similar meiosis-inhibiting activity.

Erasure of parental genomic imprints commences in PGCs at around the time of their arrival in the UGR (Szabo and Mann, 1995; Surani, 2001; Hajkova et al., 2002). However, it has not been clear whether this epigenetic event depends on induction from the UGR or is programmed autonomously in PGCs. As the offspring from PGC transplantations were viable and apparently healthy, epigenetic modifications, including erasure of parental genomic imprints, should have occurred appropriately in transplanted PGCs. This was corroborated by the normal methylation patterns exhibited in the DMRs of the *Igf2r* and *H19* genes. Because the establishment of paternal methylation proceeds after birth in the normal testis (Ueda et al., 2000), it seems unlikely that the postnatal testis has the ability to erase parental methylation. Therefore, our results suggest that PGCs may have the autonomous program for the erasure of parental methylation before reaching the UGR.

Primordial germ cell transplantation will provide a new experimental approach for the study of PGC development. Primordial germ cells harvested from embryonic lethal mutants as early as gastrulation can be traced for their differentiation capacities by transplantation into recipient testis. Similarly, PGCs manipulated in vitro, such as those cultured with growth factors or transfected with vectors (De Miguel et al., 2002; Watanabe et al., 1997), can now be assessed for their effects on subsequent differentiation in vivo. Such functional studies would help elucidate factors that regulate male germline development in mammals.

We thank Dr Masaru Okabe for kindly providing C57BL/6 Tg14 (act-EGFP) OsbY01 mice, Dr Fumitoshi Ishino for helpful advice on bisulfite sequencing, and Drs Yasuhisa Matsui and Yoshito Kaziro for critical reading of the manuscript. This research was supported by a grant from the Japanese Ministry of Education, Science, Sports and Culture.

References

Brinster, R. L. and Zimmermann, J. W. (1994). Spermatogenesis following male germ-cell transplantation. *Proc. Natl. Acad. Sci. USA* **91**, 11298-11302.

Chiarini-Garcia, H., Hornick, J. R., Griswold, M. D. and Russell, L. D. (2001). Distribution of type A spermatogonia in the mouse is not random. *Biol. Reprod.* **65**, 1179-1185.

Chuma, S. and Nakatsuji, N. (2001). Autonomous transition into meiosis of mouse fetal germ cells in vitro and its inhibition by gp130-mediated signaling. *Dev. Biol.* **229**, 468-479.

De Miguel, M. T., Cheng, L., Holland, E. C., Federspiel, M. J. and Donovan, P. J. (2002). Dissection of the c-kit signaling pathway in mouse primordial germ cells by retroviral-mediated gene transfer. *Proc. Natl. Acad. Sci. USA* **99**, 10458-10463.

de Rooij, D. G. and Russell, L. D. (2000). All you wanted to know about spermatogonia but were afraid to ask. *J. Androl.* **21**, 776-798.

Geijsen, N., Horoschak, M., Kim, K., Gribnau, J., Eggan, K. and Daley, G. Q. (2004). Derivation of embryonic germ cells and male gametes from embryonic stem cells. *Nature* **427**, 148-154.

Ginsburg, M., Snow, M. H. and McLaren, A. (1990). Primordial germ cells in the mouse embryo during gastrulation. *Development* **110**, 521-528.

Godin, I., Wylie, C. C. and Heasman, J. (1990). Genital ridges exert long-range effects on mouse primordial germ cell numbers and direction of migration in culture. *Development* **108**, 357-363.

Hajkova, P., Erhardt, S., Lane, N., Haaf, T., El-Maarri, O., Reik, W., Walter, J. and Surani, M. A. (2002). Epigenetic reprogramming in mouse primordial germ cells. *Mech. Dev.* **117**, 15-23.

Hayashi, S., Kunisada, T., Ogawa, M., Yamaguchi, K. and Nishikawa, S. (1991). Exon skipping by mutation of an authentic splice site of c-kit gene in W/W mouse. *Nucleic Acids Res.* **19**, 1267-1271.

Illmensee, K. and Stevens, L. C. (1979). Teratomas and chimeras. *Sci. Am.* **240**, 120-133.

Jiang, F.-X. and Short, R. V. (1998). Different fate of primordial germ cells and gonocytes following transplantation. *APMIS* **106**, 58-63.

Kimura, Y. and Yanagimachi, R. (1995). Mouse oocytes injected with testicular spermatozoa or round spermatids can develop into normal offspring. *Development* **121**, 2397-2405.

Labosky, P. A., Barlow, D. P. and Hogan, B. L. M. (1994). Mouse embryonic germ (EG) cell lines: transmission through the germ line and differences in the methylation imprint of insulin-like growth factor 2 receptor (Igf2r) gene compared with embryonic stem (ES) cell lines. *Development* **120**, 3197-3204.

Lee, J., Inoue, K., Ono, R., Ogonuki, N., Kohda, T., Kaneko-Ishino, T., Ogura, A. and Ishino, F. (2002). Erasing genomic imprinting memory in mouse clone embryos produced from day 11.5 primordial germ cells. *Development* **129**, 1807-1817.

Lucifero, D., Mertineit, C., Clarke, H. J., Bestor, T. H. and Tasler, J. M. (2002). Methylation dynamics of imprinted genes in mouse germ cells. *Genomics* **79**, 530-538.

Matsui, Y., Zsebo, K. and Hogan, B. L. M. (1992). Derivation of pluripotent embryonic cells from murine primordial germ cells in culture. *Cell* **70**, 841-847.

McLaren, A. (2003). Primordial germ cells in the mouse. *Dev. Biol.* **262**, 1-15.

McLaren, A. and Southee, D. (1997). Entry of mouse embryonic germ cells into meiosis. *Dev. Biol.* **187**, 107-113.

McLean, D. J., Friel, P. J., Johnston, D. S. and Griswold, M. D. (2003). Characterization of spermatogonial stem cell maturation and differentiation in neonatal mice. *Biol. Reprod.* **69**, 2085-2091.

Meistrich, M. L. and van Beek, M. E. A. B. (1993). Spermatogonial stem cells. In *Cell and Molecular Biology of the Testis* (ed. C. Desjardins and L. L. Ewing), pp. 266-295. New York, NY: Oxford University Press.

Nagano, M., Avarbock, M. R. and Brinster, R. L. (1999). Pattern and kinetics of mouse donor spermatogonial stem cell colonization in recipient testes. *Biol. Reprod.* **60**, 1429-1436.

Nocka, K., Tan, J. C., Chiu, E., Chu, T. Y., Ray, P., Traktman, P. and Besmer, P. (1990). Molecular bases of dominant negative and loss of function mutations at the murine c-kit/white spotting locus: W^{37}, W^{v}, W^{41} and W. *EMBO J.* **9**, 1805-1813.

Ogawa, T., Aréchaga, J. M., Avarbock, M. R. and Brinster, R. L. (1997). Transplantation of testis germinal cells into mouse seminiferous tubules. *Int. J. Dev. Biol.* **41**, 111-122.

Ohta, H., Tohda, A. and Nishimune, Y. (2003). Proliferation and differentiation of spermatogonial stem cells in the W/W^{v} mutant mouse testis. *Biol. Reprod.* **69**, 1815-1821.

Ohta, H., Wakayama, T. and Nishimune, Y. (2004). Commitment of fetal male germ cells to spermatogonial stem cells during mouse embryonic development. *Biol. Reprod.* **70**, 1286-1291.

Okabe, M., Ikawa, M., Kominami, K., Nakanishi, T. and Nishimune, Y. (1997). 'Green mice' as a source of ubiquitous green cells. *FEBS Lett.* **407**, 313-319.

Palermo, G., Joris, H., Devroey, P. and van Steirteghem, A. C. (1992). Pregnancies after intracytoplasmic injection of single spermatozoon into an oocyte. *Lancet* **340**, 17-18.

Resnick, J. L., Bixler, L. S., Cheng, L. and Donovan, P. J. (1992). Long-term proliferation of mouse primordial germ cells in culture. *Nature* **359**, 550-551.

Russell, L. D., Ettlin, R. A., Sinha Hikim, A. P. and Clegg, E. D. (1990). *Histological and Histopathological Evaluation of the Testis* (ed. L. D. Russell, R. A. Ettlin, A. P. Sinha Hikim and E. D. Clegg), pp. 1-40. Clearwater, FL: Cache River Press.

Shinohara, T., Orwig, K. E., Avarbock, M. R. and Brinster, R. L. (2001). Remodeling of the postnatal mouse testis is accompanied by dramatic changes in stem cell number and niche accessibility. *Proc. Natl. Acad. Sci. USA* **98**, 6186-6191.

Silvers, W. K. (ed.) (1979). *The Coat Colors of Mice*, pp. 206-223. New York, NY: Springer.

Surani, M. A. (2001). Reprogramming of genome function through epigenetic inheritance. *Nature* **414**, 122-128.

Szabo, P. E. and Mann, J. R. (1995). Biallelic expression of imprinted genes in the mouse germ line: implications for erasure, establishment, and mechanism of genomic imprinting. *Genes Dev.* **9**, 1857-1868.

Tam, P. P. and Zhou, S. X. (1996). The allocation of epiblast cells to ectodermal and germ-line lineages is influenced by the position of the cells in the gastrulating mouse embryo. *Dev. Biol.* **178**, 124-132.

Tsang, T. E., Khoo, P. L., Jamieson, R. V., Zhou, S. X., Ang, S. L., Behringer, R. and Tam, P. P. (2001). The allocation and differentiation of mouse primordial germ cells. *Int. J. Dev. Biol.* **45**, 549-555.

Toyooka, Y., Tsunekawa, N., Akasu, R. and Noce, T. (2003). Embryonic stem cells can form germ cells in vitro. *Proc. Natl. Acad. Sci. USA* **100**, 11457-11462.

Ueda, T., Abe, K., Miura, A., Yuzuriha, M., Zubair, M., Noguchi, M., Niwa, K., Kawase, Y., Kono, T., Matsuda, Y. et al. (2000). The paternal methylation imprint of the mouse H19 locus is acquired in the gonocyte stage during foetal testis development. *Genes Cells* **5**, 649-659.

Watanabe, M., Shirayoshi, Y., Koshimizu, U., Hashimoto, S., Yonehara, S., Eguchi, Y., Tsujimoto, Y. and Nakatsuji, N. (1997). Gene transfection of mouse primordial germ cells *in vitro* and analysis of their survival and growth control. *Exp. Cell Res.* **230**, 76-83.

Cell, Vol. 119, 1001–1012, December 29, 2004, Copyright ©2004 by Cell Press

Generation of Pluripotent Stem Cells from Neonatal Mouse Testis

Mito Kanatsu-Shinohara,[1] Kimiko Inoue,[5] Jiyoung Lee,[5] Momoko Yoshimoto,[4] Narumi Ogonuki,[5] Hiromi Miki,[5] Shiro Baba,[4] Takeo Kato,[4] Yasuhiro Kazuki,[7] Shinya Toyokuni,[2] Megumi Toyoshima,[3] Ohtsura Niwa,[3] Mitsuo Oshimura,[7] Toshio Heike,[4] Tatsutoshi Nakahata,[4] Fumitoshi Ishino,[6] Atsuo Ogura,[5] and Takashi Shinohara[1,8,*]

[1]Horizontal Medical Research Organization
[2]Department of Pathology and Biology of Diseases
Graduate School of Medicine
[3]Radiation Biology Center
Kyoto University
Kyoto 606-8501
[4]Department of Pediatrics
Graduate School of Medicine
Kyoto University
Kyoto 606-8507
[5]The Institute of Physical and Chemical Research
RIKEN
Bioresource Center
Ibaraki 305-0074
[6]Medical Research Institute
Tokyo Medical and Dental University
Tokyo 101-0062
[7]Department of Molecular and Cell Genetics
School of Life Sciences
Faculty of Medicine
Tottori University, Yonago
Tottori 683-8503
Japan

Summary

Although germline cells can form multipotential embryonic stem (ES)/embryonic germ (EG) cells, these cells can be derived only from embryonic tissues, and such multipotent cells have not been available from neonatal gonads. Here we report the successful establishment of ES-like cells from neonatal mouse testis. These ES-like cells were phenotypically similar to ES/EG cells except in their genomic imprinting pattern. They differentiated into various types of somatic cells in vitro under conditions used to induce the differentiation of ES cells and produced teratomas after inoculation into mice. Furthermore, these ES-like cells formed germline chimeras when injected into blastocysts. Thus, the capacity to form multipotent cells persists in neonatal testis. The ability to derive multipotential stem cells from the neonatal testis has important implications for germ cell biology and opens the possibility of using these cells for biotechnology and medicine.

*Correspondence: takashi@mfour.med.kyoto-u.ac.jp
[8]Present address: Department of Molecular Genetics, Graduate School of Medicine, Kyoto University, Kyoto 606-8507, Japan.

Introduction

Germ cells are unique in that they have the capacity to contribute genes to offspring. Although germ cells are highly specialized cells for the generation of gametes, several lines of evidence suggest their multipotentiality. For example, teratomas are tumors containing many kinds of cells and tissues at various stages of maturation, which occur almost exclusively in the gonads (Stevens, 1984). Furthermore, primordial germ cells (PGCs) from embryos between 8.5 and 12.5 days postcoitum (dpc) give rise to pluripotent cells when cultured under appropriate conditions (Resnick et al., 1992; Matsui et al., 1992). These EG cells have differentiation properties similar to ES cells isolated from inner cell mass (Martin, 1981; Evans and Kaufman, 1981). While these observations suggest that the germline lineage retains the ability to generate pluripotent cells, it has not been possible to establish pluripotent cells from normal neonatal gonads (Labosky et al., 1994).

We recently reported the in vitro culture of mouse spermatogonial stem cells (Kanatsu-Shinohara et al., 2003a), the only type of stem cell in the body that transmits genetic information to offspring (Meistrich and van Beek, 1993; de Rooij and Russell, 2000). When neonatal testis cells were cultured in the presence of glial cell line-derived neurotrophic factor (GDNF), leukemia inhibitory factor (LIF), epidermal growth factor (EGF), and basic fibroblast growth factor (bFGF), the germ cells developed uniquely shaped colonies, and the stem cells proliferated logarithmically over a 5 month period. Upon transplantation into the seminiferous tubules of infertile mice, the cultured cells produced normal sperm and offspring, and neither somatic differentiation nor teratoma formation was observed, indicating that the cultured cells were fully committed to the germ cell lineage (Kanatsu-Shinohara et al., 2003a). This was in contrast to ES cells, which produced teratoma after being transferred into seminiferous tubules (Brinster and Avarbock, 1994). Based on these results, we named these cells germline stem (GS) cells to distinguish them from ES or EG cells. Thus, GS cells represent a third method of expanding germline cells, but they are clearly distinct from ES/EG cells in their differentiation capacity.

In this manuscript, we describe the derivation of pluripotent stem cells from the neonatal mouse testis. Neonatal testis cells were cultured in conditions similar to those used for GS cell culture. In addition to the GS cell colonies, colonies indistinguishable from ES cell colonies appeared. This second cell type could be expanded selectively under culture conditions used for ES cells. Although they produced teratomas when transplanted subcutaneously or into the seminiferous tubules of the testis, they participated in normal embryonic development following injection into blastocysts.

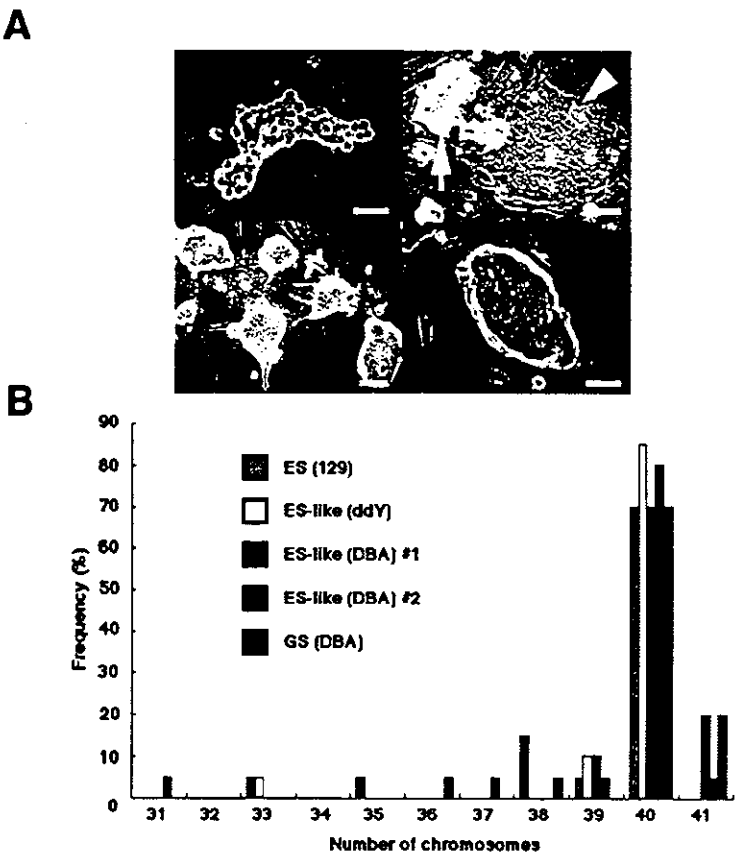

Figure 1. ES-Like Colonies from Neonatal Testis Cells

(A) Morphology of ES-like cells. (Top, left) A typical colony of GS cells. (Top, right) ES-like colony (arrow) and cultured epiblast-like colony (arrowhead), which appeared under GS cell culture conditions, at 40 days after the initiation of culture. (Bottom, left) Established culture of ES-like cells at 50 days. (Bottom, right) A typical colony of ES-like cells at 95 days.

(B) Distribution of metaphase spreads with different chromosome numbers. At least 20 cells were counted. Scale bar, 50 μm.

Results

Development of ES-Like Colonies from Neonatal Testis Cells in the Presence of Growth Factors

When neonatal ddY mouse testis cells were cultured in a primary medium containing GDNF, bFGF, EGF, and LIF, the majority of the colonies that formed had the typical appearance of GS cells, which are characterized by intercellular bridges and a morula-like structure (Figure 1A, top left) (Kanatsu-Shinohara et al., 2003a). However, we occasionally found colonies that were remarkably similar to ES cells or cultured epiblast cells (Figure 1A, top right) (Kanatsu and Nishikawa, 1996). These colonies were more tightly packed and generally appeared within 4–7 weeks after initiation of the culture (~four to seven passages). After these ES cell-like colonies appeared, they outgrew the GS cells and became the dominant population within 2–3 weeks. Although these ES-like colonies generally differentiated to lose their ES cell-like appearance after several passages under GS cell culture conditions, they retained ES-like appearance and could be selectively expanded when cultured in a secondary medium containing 15% fetal calf serum (FCS) and LIF (standard ES cell culture conditions).

After two to three passages, most colonies in the culture consisted of these ES-like colonies (Figure 1A, bottom left), which could be maintained with standard ES cell culture conditions. In contrast, GS cells could not be propagated under these conditions due to the absence of GDNF, an essential growth factor for the self-renewing division of spermatogonial stem cells (Meng et al., 2000). Cytogenetic analysis by quinacrine plus Hoechst 33258 staining showed that the ES-like cells had a normal karyotype (40, XY) in 70%–85% of metaphase spreads (Figure 1B). The morphology of the ES-like cells did not change as long as the cells were maintained in ES cell culture conditions, and they could be propagated in vitro for more than 5 months with 48 passages while maintaining an undifferentiated state (Figure 1A, bottom right). Established cultures were passed at a dilution of 1:3 to 1:6 every 3 days.

These results were reproducible; similar cells were obtained from mice with a different genotype (DBA/2), and ES-like cells were successfully established in four of 21 experiments (19%). The overall frequency of forming ES-like cells was 1 in 1.5×10^7 cells (equivalent to ~35 newborn testes). Significantly, neither GS nor ES-like cells appeared when newborn testis cells were cultured directly in ES culture conditions in at least 20 experiments. Likewise, neither GS nor ES-like cells appeared when neonatal testis cells were cultured in the presence of membrane bound Steel factor (mSCF), LIF, and bFGF (EG cell culture condition) in at least 15 experiments; the addition of GDNF was a prerequisite for the development of both GS and ES-like colonies. In addition, when CD9-selected adult spermatogonial stem cells from 3- to 8-week-old mice were cultured (Kanatsu-Shinohara et al., 2004), GS cells appeared in three of 15

experiments, but no ES-like cells appeared. We also did not observe GS or ES-like cell colonies when male genital ridges from 12.5 dpc embryos were cultured in GS cell medium in 12 experiments.

Development of ES-Like Colonies from GS Cells Derived from p53 Knockout Mice

To determine whether GS cells can convert to ES-like cells, we picked a total of 266 GS cell colonies by micromanipulation at 2 months after culture initiation. These GS cells were transferred to a 96-well plate and expanded for an additional 3 months, but none of them became ES-like cells. Although the result strongly suggested the distinct origin of ES-like cells, it was still possible that the conversion occured at lower frequency. To address this possibility, we used p53 knockout mice (Tsukada et al., 1993), which have a high frequency of testicular teratoma (Lam and Nadeau, 2003). We hypothesized that ES-like cells have a close relationship with teratoma-forming cells and asked whether established GS cells from this strain convert more easily to ES-like cells. GS cells were established from a newborn p53 knockout mouse in an ICR background. The growth speed and morphology of GS cells were indistinguishable from those of wild-type cells, and GDNF was similarly required to obtain GS cells.

Two months after culture, 30–40 GS cell colonies of undifferentiated morphology were picked by micromanipulation, transferred to a 96-well plate, and cultured in GS cell culture medium. Significantly, ES-like cells appeared in these GS cell-derived cultures in two separate experiments within 2 months, and the colonies were morphologically indistinguishable from ES-like colonies from wild-type cells. Interestingly, although ES-like cells never appeared from fully established wild-type GS cells after long-term culture, p53 knockout GS cells produced ES-like cells as long as 6 months after the initiation of culture.

Using p53 knockout mice, we also examined whether GS cells from mature testis can produce ES-like cells. Spermatogonial stem cells were collected from 3- to 8-week-old mice using anti-CD9 antibody and cultured in GS cell medium. GS cells developed in two of three experiments. GS cells of undifferentiated morphology were picked 4–7 days after culture initiation, and the colonies were expanded in vitro on mitomycin C-inactivated mouse embryonic fibroblast (MEF). In total, ES-like cells appeared in two of eight experiments within 4 weeks of culture.

Phenotypic Analysis of ES-Like Cells

To examine the phenotype of the ES-like cells, we established a population from a newborn transgenic mouse line C57BL6/Tg14(act-EGFP-OsbY01) that was bred into the DBA/2 background (designated Green). Since these Green mice express the enhanced green fluorescence protein (EGFP) gene ubiquitously, including in spermatogenic cells (Kanatsu-Shinohara et al., 2003a), cultured cells can be distinguished from feeder cells under excitation with UV light. The ES-like cells comprised a single phenotypic population by flow cytometric analysis of surface antigens (Figure 2A). They were strongly positive for SSEA-1 (ES cell marker) (Solter and Knowles, 1978), EE2 (spermatogonia marker) (Koshimizu et al., 1995), β1- and α6-integrin (GS cell marker) (Kanatsu-Shinohara et al., 2003a), CD9 (ES and GS cell marker) (Kanatsu-Shinohara et al., 2004), and EpCAM (ES and spermatogonia cell marker) (Anderson et al., 1999). The ES-like cells were weakly positive for Forssman antigen (ES cell marker) (Evans and Kaufman, 1981) and c-kit (differentiated spermatogonia marker) (Schrans-Stassen et al., 1999). In contrast, GS cells were completely negative for SSEA-1 and Forssman antigen, confirming that ES-like cells are phenotypically distinct from GS cells. GS cells from p53 knockout mice showed similar expression profile (data not shown). Although we found some expression of Forssman antigen in the neonatal testis cell population before culture, it was expressed by a non-germ cell population, and no SSEA-1-positive cells were found (Figures 2A and 2B). The ES-like cells were also strongly positive for alkaline phosphatase (ALP), which is characteristic of ES and EG cells (Resnick et al., 1992; Matsui et al., 1992) (Figure 2C).

Next, we used the reverse transcriptase-polymerase chain reaction (RT-PCR) to examine several molecules that are specifically expressed in embryonal carcinoma (EC) or ES cells. In addition to Oct-4, Rex-1, and Nanog, which are essential for maintaining undifferentiated ES cells (Pesce and Schöler, 2001; Goolsby et al., 2003; Mitsui et al., 2003; Chambers et al., 2003), the ES-like cells expressed Cripto, ERas, UTF1, Esg-1, and ZFP57 at similar levels to ES cells (Kimura et al., 2001; Takahashi et al., 2003; Okuda et al., 1998; Tanaka et al., 2002; Ahn et al., 2004). GS cells also expressed some of these molecules, but the expression was generally weaker. Significantly, we could not detect expression of Nanog in GS cells, suggesting that they have a different mechanism for self-renewal from that of ES cells (Figure 2D).

Analysis of Genomic Imprinting in ES-Like Cells

To analyze the imprinting pattern of ES-like cells, differentially methylated regions (DMRs) of three paternally imprinted regions (*H19*, *Meg3 IG*, and *Rasgrf1* regions) and two maternally imprinted regions (*Igf2r* and *Peg10* regions) were examined by bisulfite sequencing with two independent cells (Figure 3A). While the paternally imprinted regions were methylated to different degrees, the maternally imprinted regions were rarely methylated in ES-like cells. DMRs in ES cells were generally more methylated than those in ES-like cells, including maternally imprinted regions, and the DMRs of the *H19* region were methylated more extensively than the DMRs of other regions. In contrast, GS cells showed a complete androgenetic imprinting pattern: the complete methylation of both the *H19* and *Meg3 IG* DMRs and demethylation of the *Igf2r* DMR.

Next, we examined the imprint status of GS or ES-like cells from p53 knockout mice. Genomic DNA was isolated from the same cell population at four different time points during the conversion of GS cells into ES-like cells. In these experiments, the imprint status in the DMRs was determined by combined bisulfite restriction analysis (COBRA) (Xiong and Laird, 1997) (Figure 3B). As expected from the analysis of wild-type GS cells, GS

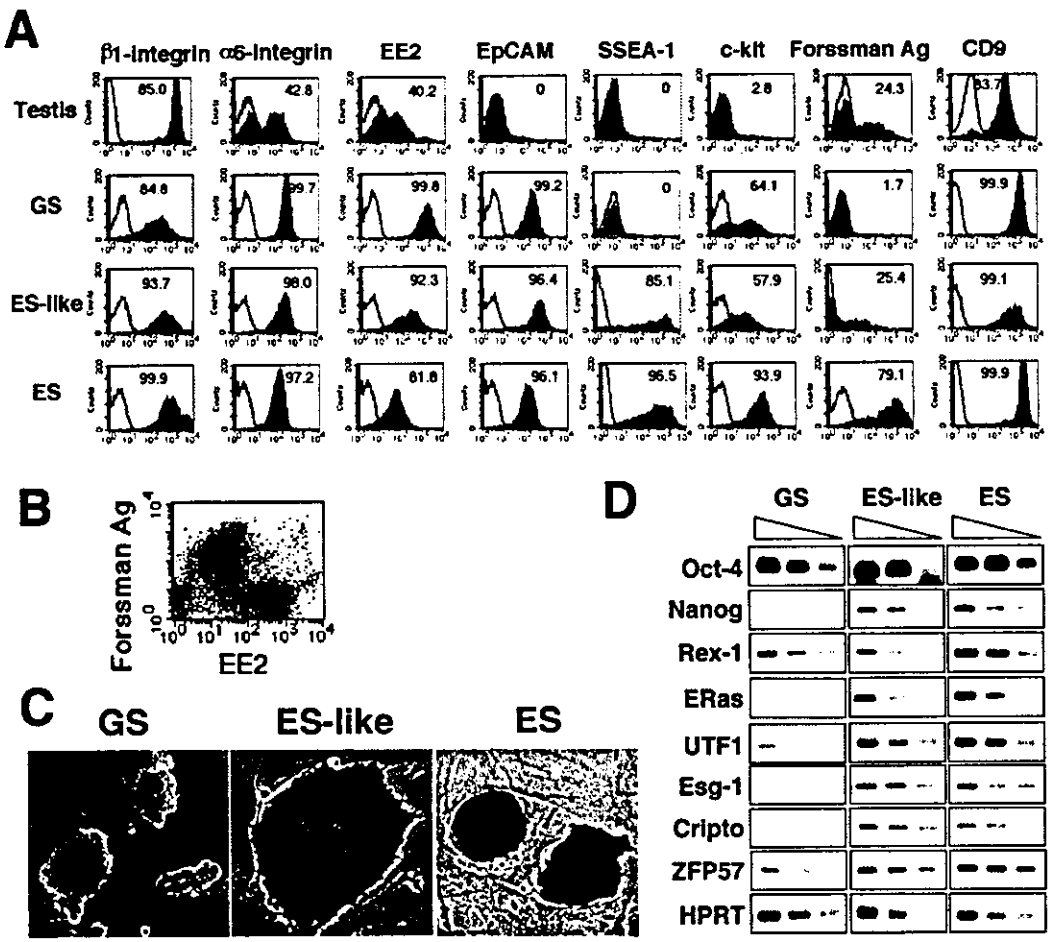

Figure 2. Phenotypic Characterization of ES-Like Cells

(A) Flow cytometric characterization of ES-like cells. Black line, control immunoglobulin; red line, specific antibody.

(B) Double immunostaining of neonatal testis cells by anti-EE2 and anti-Forssman antigen antibodies.

(C) ALP staining. GS cells (left) are weakly positive, whereas ES-like (middle) and ES cells (right) are strongly positive.

(D) RT-PCR analysis. Three-fold serial dilutions of cDNA from GS, ES-like, and ES cells were amplified with specific primers. Scale bar, 200 μm.

cells from p53 KO mice had an androgenetic imprint pattern. However, a loss of methylation in the DMRs of *H19*, *Meg 3/G*, and *Rasgrf1* regions and methylation of the DMRs in the *Igf2r* region were observed immediately after the appearance of ES-like cells. The perturbation of imprint patterns continued even when GS cells disappeared, and only the DMR of the *Peg10* region was intact, 18 days after the appearance of ES-like cells. DMR of *Oct-4* region in ES and ES-like cells were all hypomethylated, which confirms their undifferentiated state (Hattori et al., 2004) (Figure 3C).

Differentiation Potential of ES-Like Cells In Vitro and In Vivo

To determine whether ES-like cells can differentiate into somatic cell lineages, we used methods designed to induce differentiation of ES cells in vitro. ES-like cells were first transferred to an OP9 stromal feeder layer, which can support differentiation of mesodermal cells such as hematopoietic or muscle cells (Nakano et al., 1994; Schroeder et al., 2003). Within 10 days, a variety of cell types were identified including hematopoietic cells, vascular cells, and spontaneously beating myocytes (Figures 4A–4H). Hematopoiesis could also be induced when ES-like cells were cultured in methylcellulose to form embryoid bodies (Figure 4I). When we transferred ES-like cells onto gelatin-coated dishes for the differentiation of neural-lineage cells (Ying et al., 2003), they formed neurons or glial cells (Figures 4J–4L). Dopaminergic neurons were also found, albeit at low frequency (Figure 4M). When we compared the differentiation efficiency using ES cells, ES-like cells produced more glial cells than did ES cells, and there were significantly more vessel or heart muscle cell colonies from ES-like cells. However, ES-like cells could produce all of the expected lineages using protocols for ES cell differentiation (Table 1).

ES-like cells were further examined for their ability to form teratomas in vivo by subcutaneous injection into nude mice. Transplanted cells gave rise to typical teratomas in all recipients (eight of eight) by 4 weeks after transplantation (Figure 4N). The tumors contained deriv-

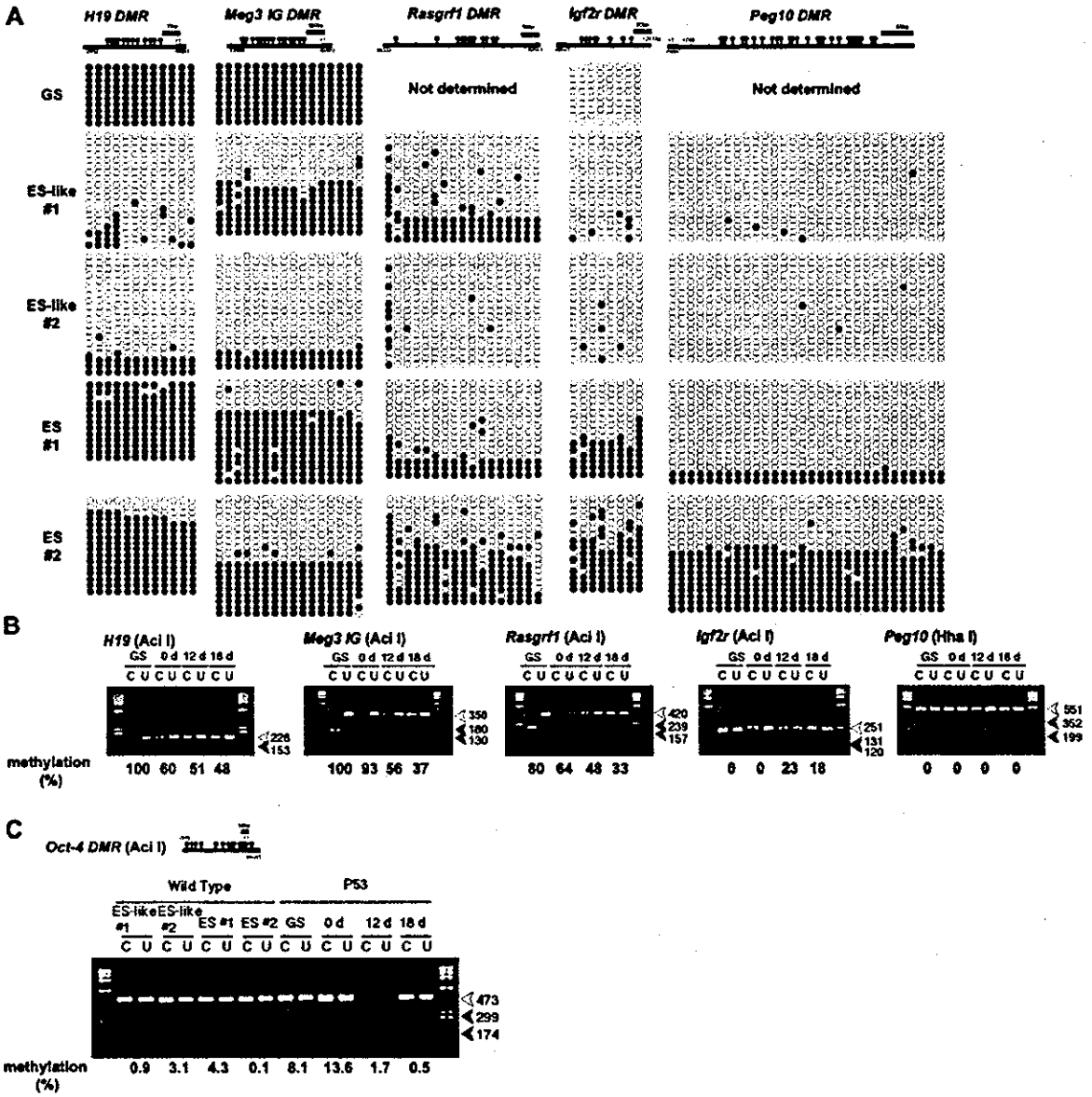

Figure 3. Analysis of Imprinting in ES-Like Cells

(A) DMR methylation of *H19*, *Meg3 IG*, *Rasgrf1*, *Igf2r*, and *Peg10* regions. DNA methylation was analyzed by bisulfite genomic sequencing. Black ovals indicate methylated cytosine-guanine sites (CpGs), and white ovals indicate unmethylated CpGs.

(B) COBRA of GS and ES-like cells from p53 knockout mice. The day when ES-like colonies were found was designated day 0, and cells were collected at the indicated time. In this culture, only ES-like cells were found by day 12.

(C) COBRA of *Oct-4* gene upstream region. Open arrowheads indicate the size of unmethylated DNA. Closed arrowheads indicate the size of methylated DNA. Enzymes used to cleave each locus are indicated in parentheses. U, uncleaved; C, cleaved.

atives of the three embryonic germ layers: squamous cell epithelium, neuroepithelium, and muscle. Similar results were obtained with three different clones or with ES-like cells from p53 knockout mice (eight of eight), and we did not observe a significant histological difference from teratomas derived from ES cells. In contrast, no tumors developed after transplantation of GS cells or fresh testis cells (data not shown).

Since the ES-like cells originated from testis, their ability to differentiate into germline cells was examined using the spermatogonial transplantation technique (Brinster and Zimmermann, 1994). This method allows spermatogonial stem cells to recolonize the empty seminiferous tubules of infertile animals and differentiate into mature sperm. We transplanted the cultured cells into immune-suppressed immature W mice (Kanatsu-Shinohara et al., 2003b). These mice are congenitally infertile and have no differentiating germ cells (Brinster and Zimmermann, 1994). One month after transplantation, all recipient animals (ten of ten) developed teratomas in

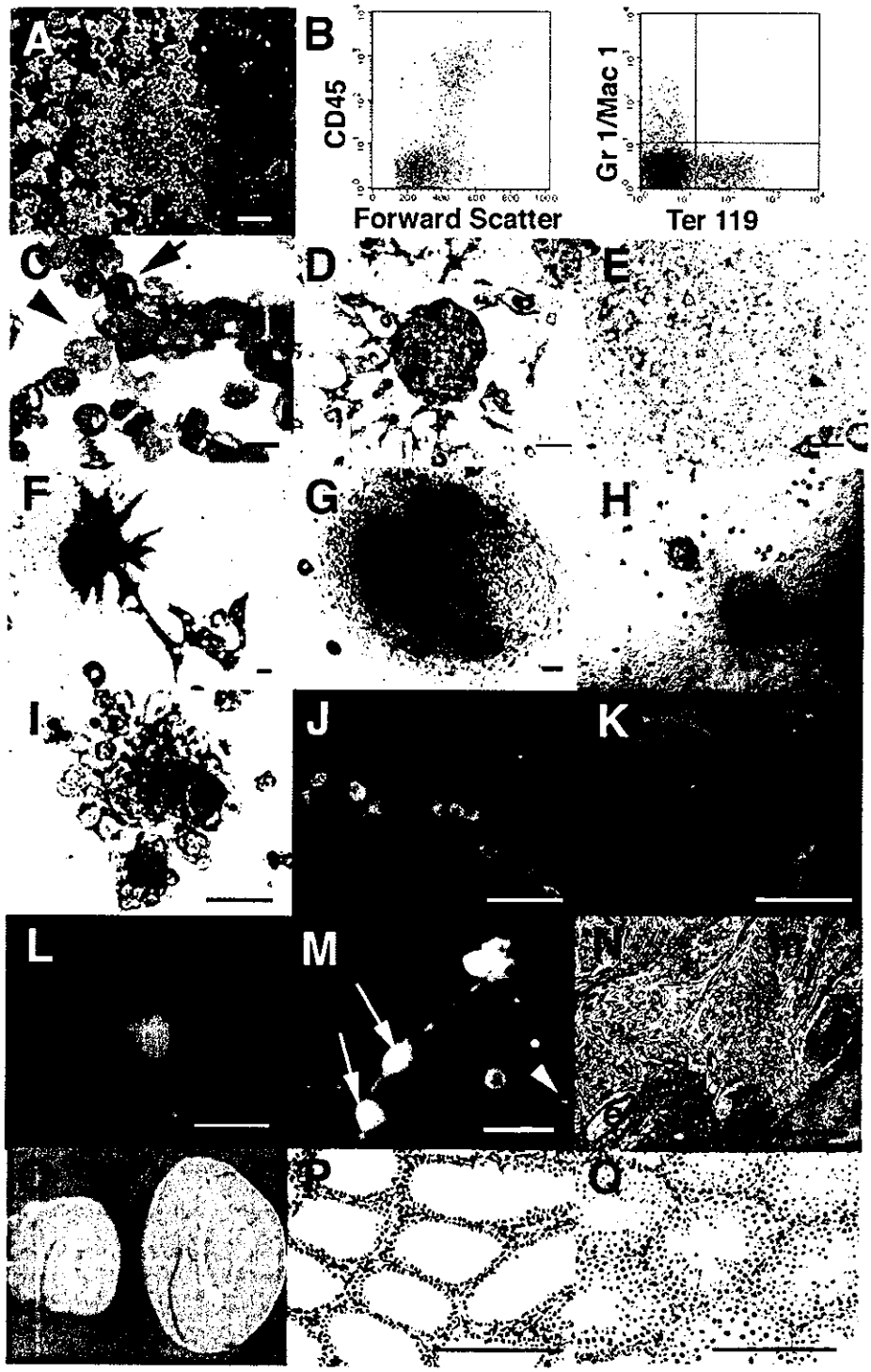

Figure 4. In Vitro and In Vivo Differentiation of ES-Like Cells

(A–H) Differentiation on OP9 cells. (A) Cobblestone formation on day 8. (B) CD45-positive hematopoietic cell development on day 7 after coculture (left). In this cell population, Gr1-positive granulocytes, Mac1-positive macrophages, or Ter119-positive erythrocytes were found (right). (C) May-Giemsa staining of harvested cells. Myeloid progenitor (arrowhead) and erythroblast (arrow) were observed. (D and E) Vascular cell differentiation. Flk-1-positive cells were sorted on day 4 after coculture, and CD31-positive (D) or VE-cadherin-positive (E) vascular cells appeared at 6 days after cell sorting. (F–H) Heart muscle differentiation. The Flk-1-positive cells were differentiated into MF20-positive (F) or cTn-I-positive (G) heart muscle at 6 days after sorting. (H) ANP-positive (blue) atrial muscle and MLC2v-positive (brown) ventricular muscle.
(I) Erythroid cells that developed from embryoid body in methylcellulose at 8 days after culture. Note the red color of the cells.
(J–M) Neuronal cell differentiation on gelatin-coated plates. Tuj-positive neurons (J) on day 5, GFAP-positive astrocytes (K) and MBP-positive

Table 1. In Vitro Differentiation of ES-Like Cells from Testis

	Hematopoiesis[a,b]			Vasculogenesis[a,c]		Neurogenesis[d]		
Cell type	Increase in cell number (fold)	Granulocyte/ Macrophage (%)	Erythrocyte* (%)	Vessel*	Heart*	Neuron*	Astrocyte*	Oligodendrocyte*
ES-like	116.7 ± 15.4	7.6 ± 0.2	19.9 ± 0.7	111.5 ± 12.0	8.0 ± 4.5	126.7 ± 14.4	34.6 ± 4.4	4.6 ± 2.5
ES cell	102.3 ± 11.6	7.6 ± 0.4	24.7 ± 0.9	49.0 ± 9.2	3.8 ± 2.0	162.2 ± 14.5	10.5 ± 3.3	0.2 ± 0.1

Values are mean ± SEM. Results from at least three experiments. ES cells were derived from 129 mice, whereas ES-like cells were derived from DBA/2 mice.

[a] Flk-1-positive cells (5×10^3) were sorted 4 days after coculture and replated on OP9 feeder in a 24-well plate.

[b] Cells were recovered 7 days after sorting and analyzed by flow cytometry. Erythrocytes, macrophages, and granulocytes were identified by anti-Ter119, anti-Mac1, and anti-Gr1 antibodies, respectively.

[c] Numbers of positive cells in each well, 8 days after sorting. Vascular cells were determined by the uptake of DiI-acetylated low-density lipoprotein. Heart muscle colonies were identified by counting beating colonies.

[d] Cells (2.5×10^4) were plated on gelatin in a 48-well plate, and numbers of positive cells per cm^2 were determined by immunocytochemistry 5 (neuron) or 7 (astrocytes or oligodendrocytes) days after plating. Neurons were identified by anti-Tuj antibody, whereas astrocytes and oligodendrocytes were identified by anti-GFAP or anti-MBP antibodies, respectively. Dopaminergic neurons were produced ~10 cells per well.

* Statistically significant by Student's t test ($p < 0.05$).

the testis. The seminiferous tubules were disorganized, and no sign of spermatogenesis was found in histological sections. The cell composition found in the teratomas was similar to that of tumors that developed after subcutaneous injection (data not shown). In contrast, both wild-type and p53 KO GS cells produced normal spermatogenesis when transplanted into the seminiferous tubules (Figures 4O–4Q).

Contribution of ES-Like Cells to Normal Embryonic Development after Blastocyst Injection

Finally, we microinjected ES-like cells into blastocysts to examine whether they can contribute to chimeras in vivo. Five to fifteen cells were injected into C57BL/6 blastocysts. The ratio of euploid cells, which significantly influences the rate of chimerism or germline transmission (Longo et al., 1997; Liu et al., 1997), was 70% at the time of injection.

Some of the recipient animals were analyzed at 12.5 dpc to look for chimerism, and others were allowed to develop to term. Chimerism was observed in 25% (three of 12) of the 12.5 dpc embryos (Figure 5A) and in 36% (13 of 36) of the newborn animals (Figure 5B), as judged by the expression of EGFP observable under UV illumination. Chimerism was also confirmed by the coat color at mature stage (Figure 5C). We found six dead fetuses that showed EGFP expression, and some embryos were partially or completely absorbed. The pattern of contribution was similar at both stages analyzed; EGFP-positive donor cells were found in the central nervous system, liver, heart, lung, somites, intestine, and other tissues, including the yolk sac and chorionic membrane of the placenta (Figures 5D–5I).

Since donor cells were also found in the testis of a chimeric animal at 6 weeks of age (Figure 5J), we performed microinsemination to obtain offspring. Round spermatids were collected and microinjected into C57BL/6 × DBA/2 (BDF1) oocytes. Of 81 cultured embryos, 64 (79%) developed into 2-cells and were transferred into five psudopregnant females. Eighteen (22%) embryos were implanted, and one of the two offspring from a recipient mouse showed EGFP fluorescence, indicating the donor origin (Figure 5K). Interestingly, while control ES cells showed wide contribution to embryos, no donor cell contribution was observed in experiments using GS cells (Table 2).

To determine the full developmental potential of ES-like cells, we used tetraploid complementation technique (Nagy et al., 1993). This technique allows the production of live animals that consist entirely of donor ES cells. A total of 92 tetraploid embryos were created by electrofusion, aggregated with ES-like cells, and transferred to pseudopregnant ICR females. When some of the recipient animals were sacrificed at 10.5 dpc, we found one normal-looking fetus and several resorptions with normal placentas. The fetus showed some growth retardation but clearly expressed the EGFP gene throughout its body, including the yolk sac (Figure 5L), indicating that it was derived from donor ES-like cells. However, none of the pseudopregnant mothers sired live offspring from both ES-like and ES cells.

Discussion

The results of our experiments revealed the presence of multipotential stem cells in the neonatal testis. Although some cases of the "stem cell plasticity" phenomenon

oligodendrocytes (L) on day 7 after induction. TH and Tuj-double positive dopaminergic neurons (arrow) appeared among Tuj-positive neurons (arrowhead) (M).

(N) Section of a teratoma under the skin. The tumors contained a variety of differentiated cell types, including muscle (m), neural (n), and epithelial (e) tissues.

(O–Q) Spermatogenesis from p53 knockout GS cells. (O) A macroscopic comparison of untransplanted (left) and transplanted (right) recipient testes. Note the increased size of the transplanted testis. (P and Q) Histological appearance of the untransplanted (P) and transplanted (Q) W testes. Note the normal appearance of spermatogenesis (Q). Color staining: Cy3, red (J–M); Alexa Fluor 488, green (M). Scale bar, 50 μm (A, D–I, J, K, and M), 20 μm (C and L), 200 μm (N, P, and Q), 1 mm (O).

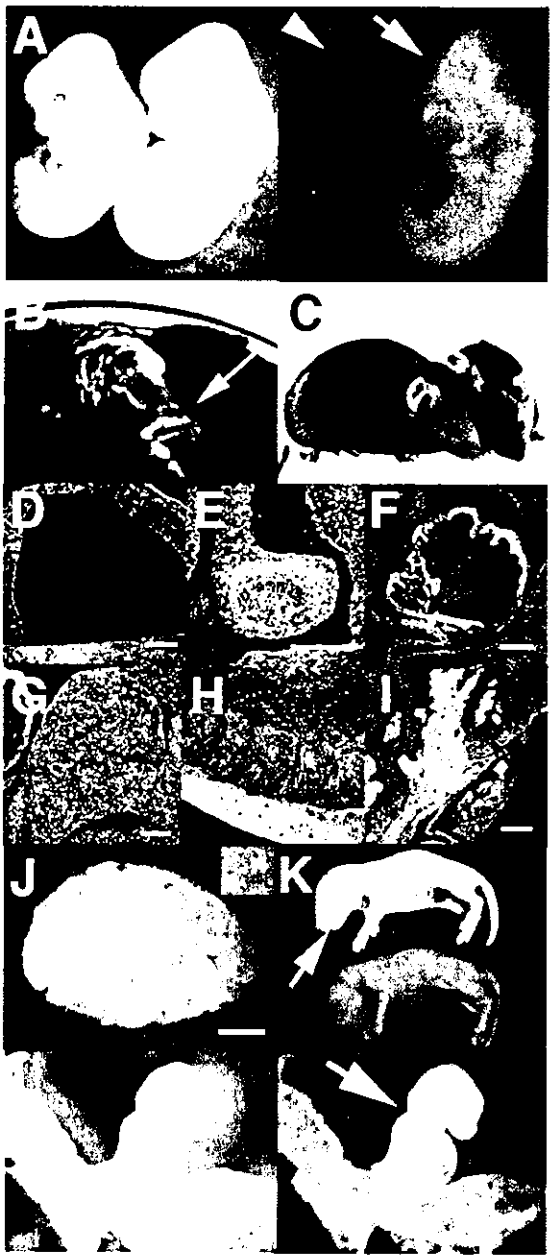

Figure 5. Production of Chimeric Animals

(A) A 12.5 dpc chimeric embryo (arrow) showing fluorescence under UV light. No fluorescence was observed in a control embryo (arrowhead).

(B) A newborn chimeric animal (arrow) showing fluorescence.

(C) Mature chimeric animals. Note the donor cell-derived coat color (cinnamon).

(D–I) Parasagittal section of a 12.5 dpc chimeric embryo. Fluorescence was observed in the brain (D), intestine (E), heart (F), liver (G), lower spinal cord (H), and placenta (I).

(J) A testis from a chimeric mouse showing fluorescence. EGFP expression was observed in some germ cells in the testis cell suspension (inset).

(K) Offspring derived from a chimera. One of the offspring showed fluorescence, confirming the donor origin (arrow).

(L) A 10.5 dpc embryo (arrow) and yolk sac produced from an aggregation of ES-like cells with tetraploid embryo showing fluorescence. No fluorescence was observed in the placenta (arrowhead). Counterstained with propidium iodide (PI) (D–I). Color staining: EGFP, green (A, B, and D–L); PI, red (D–I). Scale bar, 100 μm (D–I), 1 mm (J).

have been attributed to cell fusion (Wagers and Weissman, 2004), our case cannot be explained by the same mechanism because the ES-like cells formed teratomas after subcutaneous transplantation. These ES-like cells from the testis can be considered the neonatal counterparts of ES/EG cells. The result was unexpected, since PGCs become resistant to experimental teratocarcinogenesis or EG cell formation after 13.5 dpc (Stevens, 1984; Labosky et al., 1994). To our knowledge, EG cells are the only example of the isolation of multipotent stem cells from primary germ cells (Resnick et al., 1992; Matsui et al., 1992). EG cells were derived from primary germ cells harvested from 8.5 to 12.5 dpc fetuses and cultured in vitro with a mixture of mSCF, LIF, and bFGF. However, pluripotent cells could not be isolated from neonatal germ cells using the same culture conditions (Labosky et al., 1994), except when cells from teratomas were used (Robertson and Bradley, 1986). ES-like cells are unlikely to be derived from teratoma cells for two reasons. First, the frequency of derivation of ES-like cells in our study was significantly higher than the negligible rate of spontaneous teratoma formation in strains other than 129 and A/He mice (one teratoma out of 11,292 males in 129 hybrid backgrounds) (Stevens and Mackensen, 1961). Second, growth factor supplementation was essential for the establishment of ES-like cells. In fact, few EC cell lines have been obtained from spontaneously occurring teratocarcinomas (Robertson and Bradley, 1986). These findings strongly suggest that the ability to become multipotent stem cells persists in neonatal testis. Based on the results reported here, we propose to name these ES-like cells multipotent germline stem cells, or mGS cells, to distinguish them from GS cells, which can differentiate only into germline cells (Kanatsu-Shinohara et al., 2003a).

An important question that arises from this study is the origin of mGS cells. One possibility is that they appear independently from GS cells and originate from a population of undifferentiated pluripotent cells that persist in the testis from the fetal stage. Although EG cells have been established from ~12.5 dpc PGCs (Matsui et al., 1992; Labosky et al., 1994), cells with similar characteristics might remain in neonatal testis and produce ES-like cells. Indeed, the results of the imprinting analysis of wild-type mGS cells suggest a distinct origin for mGS cells. In male germ cells, genomic imprinting is erased during the fetal stage, and male-specific imprinting begins to be acquired around birth in prospermatogonia and is completed after birth (Davis et al., 1999, 2000; Kafri et al., 1992). While GS cells had a typical androgenetic imprinting pattern, the imprinting pattern of mGS cells clearly differed from those of androgenetic germ cells or somatic cells, which suggested that mGS cells originate from partially androgenetic germ cells that have undergone imprint erasure.

Another possibility is that mGS cells are derived from spermatogonial stem cells and that the ability to become multipotential cells may be one of the general character-

Table 2. Contribution of ES-Like Cells to Embryonic Development

Type of Cells	Number of Embryos Transferred	Number of Recipients	Number of Pups Born[a]	Number of Live Pups[b]	Chimera (%)	
					Male	Female
ES-like	193	11	54	36	9/22 (41)	4/14 (29)
ES	91	14	14	4	2/2 (100)	2/2 (100)
GS	124	7	28	16	0/8 (0)	0/8 (0)
4n rescue ES-like	92	4	0	NA	NA	NA
4n rescue ES	30	2	0	NA	NA	NA

NA, not applicable.
[a]In some experiments, fetuses were delivered by cesarean section at 19.5 dpc.
[b]Number of live pups on the next day after birth.

istics of germline cells. Possibly, the interaction with Sertoli cells normally directs germ cells to spermatogenesis and inhibits multilineage differentiation in the testis. However, when germline cells are continuously stimulated to expand in the absence of Sertoli cells, as in our culture conditions, germ cells may be released from this inhibition and some of the cells converted to pluripotent cells. Teratogenesis from germline cells is susceptible to environmental influences; for example, teratoma formation can be significantly enhanced (~10-fold) in vivo by ectopic transplantation of the fetal genital ridge (Stevens, 1984). As PGCs can become pluripotential only after in vitro culture and cytokine supplementation was also necessary for EG cell conversion (Matsui et al., 1992; Resnick et al., 1992), growth stimulation and release from somatic cells may modify the differentiation program of germline cells.

Several lines of evidence in our study provide support for the multipotential nature of spermatogonial stem cells. First, we did not find PGC-like germ cells in the neonatal testis, and we failed to induce mGS cells from neonatal testis in EG cell culture conditions (mSCF + LIF + bFGF). Therefore, the mGS cells arose through a different mechanism from that of EG cells, and the results suggest that PGC-like cells in neonatal testis, if any, are not responsible for the generation of mGS cells. Second, results of p53 knockout mouse experiments showed that mGS cells develop from GS cells. The use of the p53 knockout mouse was based on previous studies that showed an increased frequency of teratoma in this strain; it is estimated that loss of the *p53* gene results in a 100-fold increase in the susceptibility to testicular teratoma (Lam and Nadeau, 2003). Nevertheless, GS cells from this strain were phenotypically similar to wild-type spermatogonia and could produce normal-appearing spermatogenesis when transferred into seminiferous tubules. In this sense, they are indistinguishable from wild-type GS cells and fulfill the criteria for spermatogonial stem cells. Using this model, we found that the partial androgenetic imprint in mGS cells occurred with loss of the androgenetic imprint in GS cells. Perhaps the same is true of wild-type mGS cells; the partial androgenetic imprint patterns may not indicate the origin of mGS cells directly but rather reflect epigenetic instability in vitro, as reported for ES/EG cells (Labosky et al., 1994; Dean et al., 1998; Humpherys et al., 2001). Although these results are based on a mutant mouse model, they strongly suggest that GS cells are multipotential or can acquire multipotentiality by loss of a single gene. Spontaneous teratomas in mice occur almost exclusively in the 129/Sv background and are considered to develop from PGCs (Stevens, 1984). However, our results strongly suggest that spermatogonial stem cells are multipotential.

Interestingly, the acquisition of multipotentiality in mGS cells was concurrent with the loss of spermatogonial stem cell potential. Despite their testicular origin, mGS cells formed teratomas in the seminiferous tubules, indicating that this environment was no longer sufficient for spermatogenesis after the cells became pluripotent. This contrasts with GS cells, which produce spermatogenesis on transfer to the seminiferous tubules (Kanatsu-Shinohara et al., 2003a). Therefore, mGS cells are more closely related to ES/EG cells in terms of cell function. The reason for the loss of spermatogonial stem cell potential is unknown; however, we speculate that it may be related to the loss of responsiveness to GDNF during the course of the establishment of mGS cells, as GDNF is essential for the self-renewing division of spermatogonial stem cells (Meng et al., 2000). Another question that remains to be answered is why GS cells converted to mGS cells only at early passages. In our experiments, mGS cells appeared within 7 weeks of culture initiation but not at later stages. Once established, however, GS cells were stably committed to the germline, because we did not observe any mGS cell conversion when they were expanded in large-scale culture or transplanted in vivo. The loss of multipotentiality might be ascribed to the nonoptimal culture condition; it is widely known that ES cells differentiate easily and lose germline potential in the absence of LIF (Smith, 2001). Likewise, germline cells may tend to lose somatic cell potential in nonoptimal culture conditions. In this sense, it is interesting that, in contrast to mGS cells from wild-type mice, mGS cells developed in the long-term in p53 knockout mice. Although the mechanism for the maintenance or loss of multipotentiality of germline cells is currently unclear, the results suggest that this gene is involved in these processes, and GS cells from p53 knockout mice may be useful for analyzing how germline cells retain multipotentiality.

The most striking result from our experiments is the contribution of mGS cells to normal embryo development. Donor cell makers were present in various parts of the body, including the germline cells. These results demonstrate that mGS cells not only produce tumors but also can contribute to normal embryonic development. However, the function of the cells may not be completely